AD-A040 836 ARMY MISSILE RESEARCH AND DEVELOPMENT COMMAND REDSTO--ETC F/G 17/8
FUNDAMENTALS IN VISIBILITY.(U)
FEB 77 H B HOLL

UNCLASSIFIED DRDMI-TR-77-1 NL

| OF |
ADA
040836

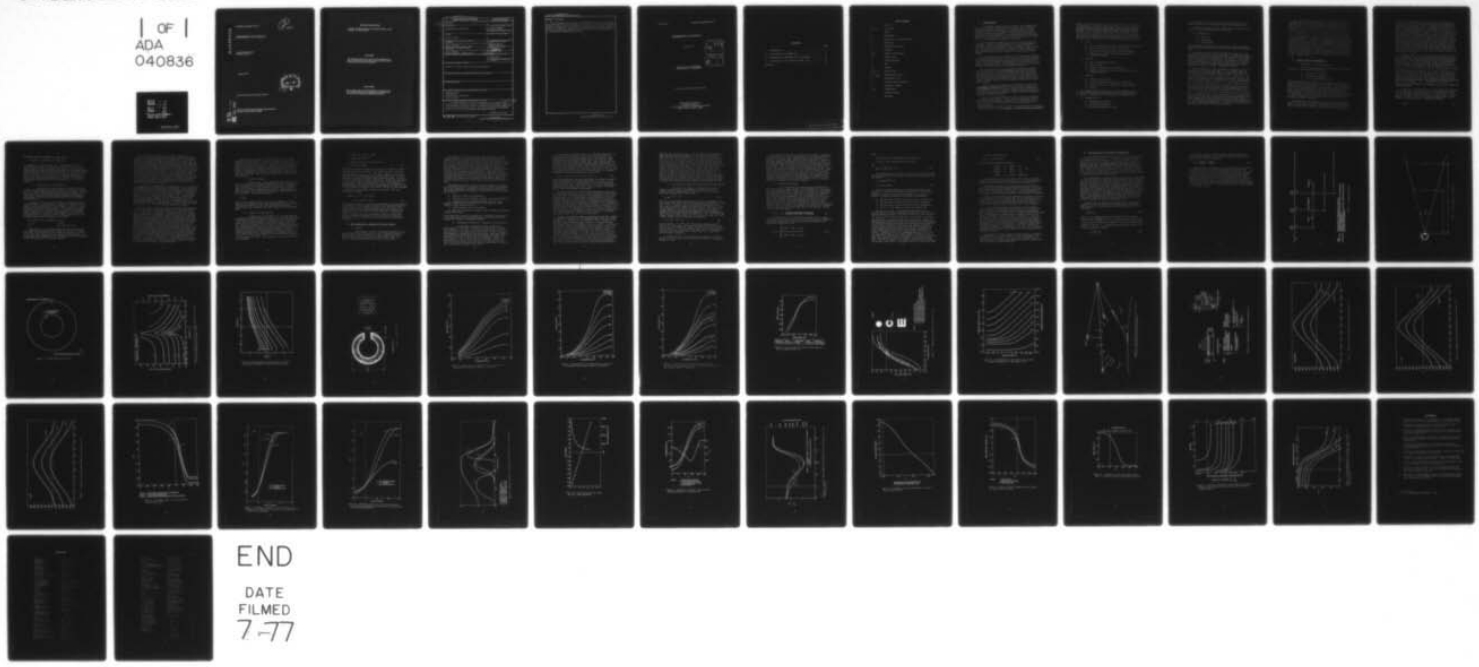

END

DATE
FILMED
7-77

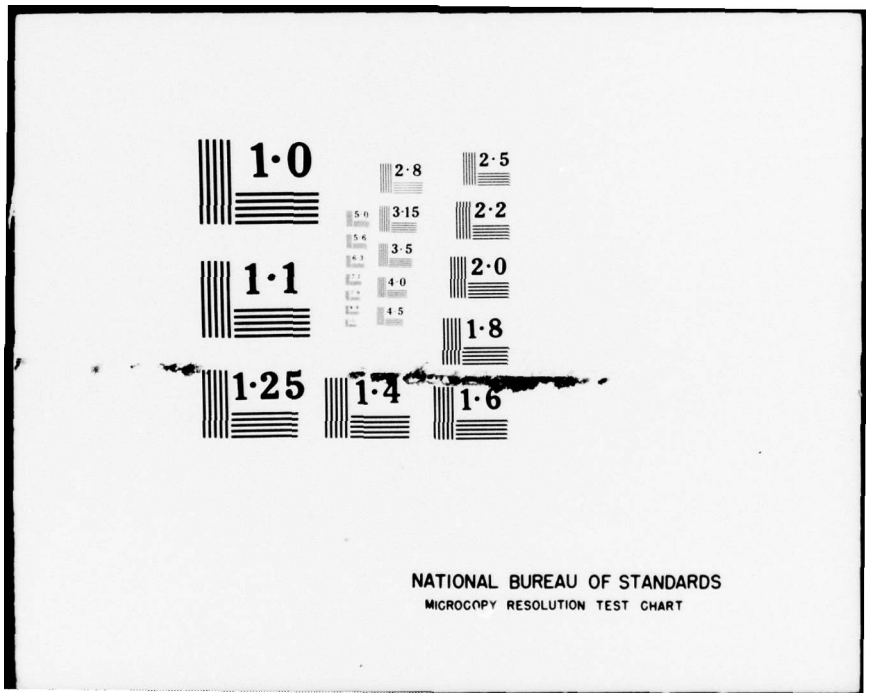
1·0
2·8
2·5
3·15
2·2
3·5
1·1
2·0
4·0
1·8
1·25
1·4
1·6
NATIONAL BUREAU OF STANDARDS
MICROCOPY RESOLUTION TEST CHART

TECHNICAL REPORT TR-77-1

FUNDAMENTALS IN VISIBILITY

Physical Sciences Directorate
Technology Laboratory

February 1977

Approved for public release; distribution unlimited

US Army Missile Research and Development Command
Redsteon Arsenal, Alabama 35809

DISPOSITION INSTRUCTIONS

DESTROY THIS REPORT WHEN IT IS NO LONGER NEEDED. DO NOT RETURN IT TO THE ORIGINATOR.

DISCLAIMER

THE FINDINGS IN THIS REPORT ARE NOT TO BE CONSTRUED AS AN OFFICIAL DEPARTMENT OF THE ARMY POSITION UNLESS SO DESIGNATED BY OTHER AUTHORIZED DOCUMENTS.

TRADE NAMES

USE OF TRADE NAMES OR MANUFACTURERS IN THIS REPORT DOES NOT CONSTITUTE AN OFFICIAL INDORSEMENT OR APPROVAL OF THE USE OF SUCH COMMERCIAL HARDWARE OR SOFTWARE.

UNCLASSIFIED

SECURITY CLASSIFICATION OF THIS PAGE (When Data Entered)

REPORT DOCUMENTATION PAGE

READ INSTRUCTIONS BEFORE COMPLETING FORM

1. REPORT NUMBER: TR-77-1	2. GOVT ACCESSION NO.
3. RECIPIENT'S CATALOG NUMBER	
4. TITLE (and Subtitle): FUNDAMENTALS IN VISIBILITY,	5. TYPE OF REPORT & PERIOD COVERED: Technical Report,
	6. PERFORMING ORG. REPORT NUMBER
7. AUTHOR(s): Herbert B. Holl	8. CONTRACT OR GRANT NUMBER(s)
9. PERFORMING ORGANIZATION NAME AND ADDRESS: Commander, US Army Missile Research and Development Command, Attn: DRDMI-TR, Redstone Arsenal, Alabama 35809	10. PROGRAM ELEMENT, PROJECT, TASK AREA & WORK UNIT NUMBERS: DA 1L161102AH49, AMCMS 611102.H490011
11. CONTROLLING OFFICE NAME AND ADDRESS: Commander, US Army Missile Research and Development Command, Attn: DRDMI-TI, Redstone Arsenal, Alabama 35809	12. REPORT DATE: February 1977 13. NUMBER OF PAGES: 53
14. MONITORING AGENCY NAME & ADDRESS (if different from Controlling Office)	15. SECURITY CLASS. (of this report): UNCLASSIFIED 15a. DECLASSIFICATION/DOWNGRADING SCHEDULE

16. DISTRIBUTION STATEMENT (of this Report)

Approved for public release; distribution unlimited.

17. DISTRIBUTION STATEMENT (of the abstract entered in Block 20, if different from Report)

18. SUPPLEMENTARY NOTES

19. KEY WORDS (Continue on reverse side if necessary and identify by block number)

Visibility acuity
Light sources
Brightness and illumination
Sky and terrain

20. ABSTRACT (Continue on reverse side if necessary and identify by block number)

Any defense depends on a very fast perception of the enemy's actions. The best weapon will be of no use if it cannot be employed early enough. The understanding of the physics related to visibility is of definite importance in the field application of lasers. The issue of visibility measurements becomes crucial in the Submillimeter Wave Research Project.

ABSTRACT (Continued)

DD FORM 1 JAN 73 1473 EDITION OF 1 NOV 65 IS OBSOLETE

UNCLASSIFIED

SECURITY CLASSIFICATION OF THIS PAGE (When Data Entered)

410217

ABSTRACT (Concluded)

It is the purpose of this report to outline research results which define the fundamentals of visibility acuity. The report will deal with the following subjects: visual acuity of the human eye; determination of minimum visibility; acuity and sensitivity; visibility of light sources; brightness and illumination of sky and terrain and changes from day to night; the color of skylight; and the variation of visibility during a day.

February 1977

TECHNICAL REPORT TR-77-1

FUNDAMENTALS IN VISIBILITY

Herbert B. Holl

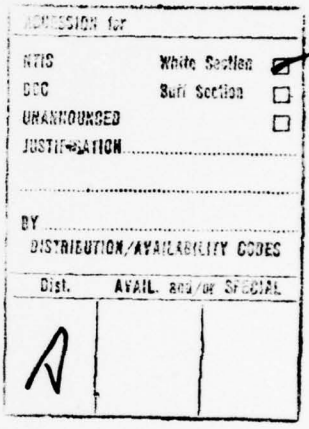

DA Project No. 1L161102AH49
AMCMS Code No. 611102.H490011

Approved for public release; distribution unlimited

Physical Sciences Directorate
Technology Laboratory
US Army Missile Research and Development Command
Redstone Arsenal, Alabama 35809

CONTENTS

LIST OF SYMBOLS

C	Contrast
$C = F.I.$	Color index
P	Object
R	Reflectance
S	Snellen unit = (visual acuity)
U	Background
a	Absorption coefficient
d	Distance
$e(\lambda)$	Spectral sensitiviness
$h_{\odot}$	Height of sun
m	Stellar magnitude
t	Time
$2y$	Diameter
$Y = 2\omega$	Angle of view
$Y = 2\omega_{min}$	Minimum angle of view
δ	Declination of sun
ϵ	Relative contrast threshold
φ	Geographic latitude
$\phi(\lambda)$	Transparency
σ	Contrast function
τ	True time

I. INTRODUCTION

Fundamental research work on visibility is, in general, done for clinical, military, and astronomical purposes, and to a greater extent in meteorology and geophysics. Astronomers are particularly interested in this field of science because the human eye is a very important instrument in observation. In geophysics and meteorology, researchers are less interested in the detailed knowledge of the parameters which effect visibility per se; their interest is to relate visibility to the parameters of atmospheric properties.

Any object becomes visible only if there is a contrast with its background. Because any defense depends on a very fast perception of the enemy's action, the determination of the contrast threshold of the human eye has been frequently an object of research effort for military purposes, particularly during the last war. Basic research has been proceeding for many years, especially in Europe and the United States.

In the United States, the facilities of the Louis Comfort Tiffany Foundation, Oyster Bay, New York, which was an art school in peace time, were completely engaged during the war years under a contract with the Office of Scientific Research and Development. A part of the war program was the determination of the contrast threshold of the normal human observer under a wide variety of experimental conditions.*

On the other side of the ocean a similar program was conducted under the direction of the Heereswaffenamt (which also directed the development of the V2 under Gen. Dornberger and Wernher von Braun). The Heereswaffenamt also employed the researcher of the Observatory of the Friedrich Schiller Universität, Jena/Th., now East Germany. The results obtained here are scattered in internal reports and relatively unknown journals; therefore, they were rarely considered in the dominant literature.

Visibility is more or less precisely defined in the literature. The Glossary of Meteorology defines it as the greatest distance in a given direction at which it is just possible to see and identify with the unaided eye, (a) in the daytime a prominent dark object against the sky at the horizon, and (b) at night, a known, preferably unfocussed, moderately intense light source.

First, the term "visibleness" as it will be used in the remainder of the text will be defined. In this concept, the human eye plays a dominant part; its efficiency, sensibility, and adaptability must be taken into account. In practice, it is the task of an observer to

*For more details, the reader is refered to the publications of Blackwell and Duntley, and to the book Middleton: Visiblity through the Atmosphere.

describe precisely, unequivocally, and accurately what he observes, and to accomplish this immediately after observation. This is a very demanding requirement to place on a human being. Further, an object must be defined. In order to arrive at the fundamentals, actual objects must be compared with well-defined reference objects with respect to shape, surface, contour, cross section, and color. Without claiming completeness, some of the parameters which are fundamental to the perception of an object and those which influence the observation are listed as follows. The factors with similar kinds of characteristics are grouped together.

a) Group I

1) For the detection of an object, a certain time is required.
2) The object must exceed a certain visual angle.
3) The background must be beyond a certain brightness.
4) There must be a certain contrast between object and background luminance.

b) Group II

1) Color of background and object.
2) Shape of object.
3) Intensity distribution of the background.
4) Distance of the object from the fixed point of the eye (visual distance).

c) Group III

1) Training of the observer.
2) Visual performance of the observer (normal eye).
3) Careful adaption to the brightness of the background.
4) Fatigue.

The process, from first detection to precise recognition with the eye, is a physiologically controlled event with increasing demands on the observer. The process can be divided into the following steps:

a) Classification A

1) Observation of existence.
2) Approximate recognition.
3) Precise understanding of object.

With this classification physical and physiological aspects are considered together, based on different levels of intellectual power.

For military purposes a similar classification is already in use, which will be called Classification B as follows:

b) Classification B

1) Detection.

2) Acquisition.

3) Identification.

Additional military actions, such as beam-riding, tracking, illumination, and range determination, may start during or after the acquisition game.

The different phases of object identification Steps 2 and 3 of Classification A take place with elapsed time. In scientific research studies, it is customary to determine "visibility acuity" and to find the threshold intensities for different kinds of objects. In such experiments, the observer is not time-limited. The remainder of this report will therefore present only those results where time is not involved. Steps 2 and 3 will be illustrated as they occur when an air target is approaching an observer. Figure 1 illustrates this case.

The arrow from left to right represents the time in which the process occurs. At the origin the time is $t = 0$. A chosen object is approaching from a far distance, and if it follows the shortest path the background conditions always remain the same. At the time $t = t_1$ the observer learns that there is something in his field-of-view. Any change of his observation is caused only by the object. With elapsed time the observer sees more. At the time $t = t_2$ he recognizes the contour of the object, and at the time $t = t_3$ he sees details of the surface. Besides this observation, the observer may also have the task of starting actions toward the threat. The same parameters as listed in Classification B are those which are predominant at times t_1, t_2, and t_3. The upper part of Figure 1 represents a case where the observer has the information that a target is approaching in a well-defined path. As shown in the lower part of the figure, an observer responsible for a broader angular sector will need more time with the lower values of t even with additional information (early warning), and with greater values of t without additional information. On the basis of this description and general observation, the following are noted:

1) The first detection depends on the distance and the size of the observed object, which finally results in the angle of view, i.e., the angle under which the object occurs to the observer during the flight (Figure 2). For the first detection, there exists a minimum angle $2\omega_{min}$, which occurs with an object of the diameter $2y_1$ at the distance d_1, and with an object of the diameter $2y_2$ at the distance d_2, etc. This angle has to be met or exceeded as a minimum for visibility.

2) From daily life it is obvious that to read a book a certain amount of illumination is necessary. However, the human eye is limited to a certain range. If the light is too intense, it is blinding. The reaction of the eye is that the pupil becomes smaller; if the disturbance is too severe, the eye is unable to read because the background is too bright. An opposite case occurs after sunset. At a certain time during the twilight it becomes difficult to read. In order to receive more light the pupil increases its diameter until it is unable to distinguish details. This happens when the sun is approximately 7° under the horizon. In the first case, the contrast between the letters (object) and the paper (background) is very great, whereas in the second case, there is only a slight contrast.

II. VISUAL ACUITY OF THE HUMAN EYE

A. Determination of Minimum Visibility

In the previous discussion the visibility process was subdivided into three steps (Classification A):

1) Observation of existence.

2) Approximate recognition.

3) Precise understanding of object.

Objects with extreme surface forms, e.g., those not of a square measure, such as long bars will be excluded. Then it follows that the first detection does not depend on the form of the object. The circular disk, Figure 3, which is characterized by its diameter, was adopted as a test figure. It is beyond the scope of this study to determine to what extent results would change if extreme shapes like bars or wires were being considered. The following results are based on References 1 through 7. Useful results are only those from visibility tests where observers with normal eyes and with certain experience were used [1, 2, and 7]. All data were received binocularly.

The perception of the existence of an object is physically determined by the contrast in brightness (measuring of a contrast threshold) where it becomes visible against a well-defined uniform background. In order to observe circular disks of different illuminance and diameters

in contrast to backgrounds of various degrees of illuminance, one method is to project two concentric disks of different brightness on an ideal reflecting screen of paper. The larger disk represents the background (whose luminance is U); the smaller disk represents the object or target (of luminance P). At a distance of 3.44 m, a circular disk of 1-mm diameter subtends an angle of 1 min. The contrast C between P and U is defined by the ratio C = P/U, which varies between 0 (total darkness of P) and large positive values. The contrast C at which an object of given diameter is just barely recognizable can be observed in the following way. The illuminance of the field U is kept constant by a known source; the illuminance of the field P is decreased very slowly until the two blend together. There is no sharp border between visible and invisible; rather, there is a transition area in which the human eye sometimes sees an object and sometimes does not. In the studies from which these results were taken, it was decided to consider an object as detected if the observer failed in no more than one out of ten tests to find the object under the same conditions. In this case $C > 1$ is used.

The opposite case, $C < 1$, was also employed; the numerical results were not identical. Because the observer was not limited by time in these research tests, the results represent the maximum visual performance of the eye. Such tests have been performed by several research institutes during the past three decades. Figure 4 illustrates the results obtained by the Observatory Jena, and presents the relationship between contrast and illuminance of U for the angles of view $\gamma = 2\omega_{min} = 0.5$, 1, 2, 5, 10, and 20 minutes. For each of the previously mentioned angles, there is only one curve in each of the areas $C < 1$ and $C > 1$. For greater values of U, these curves become more and more symmetrical with respect to the straight line $C = 1$. The area below a specific curve illustrates the conditions of the cases in which the object is invisible. The upper area represents the conditions under which an object becomes visible. This visibility increases as the illumination on U is increased. If the illuminance is so high that the luminance exceeds 10^5 apostilb, the visibility will decrease because the eye becomes blinded.

The condition $C < 1$ illustrates to a certain degree the cases where the background is the daytime sky; then $C < 1$ means a passive target, which is less bright than the background. The condition $C > 1$ represents an illuminated target, which case occurs after sunset. In these studies, the case $C > 1$ was of more interest than the case where the contrast was smaller than unity. Contrast is defined by

$$C = \frac{P - U}{U} \tag{1}$$

and Brigg's two-place logarithms are used, namely:

$$\sigma = \log^{10} C = \log^{10} \frac{P - U}{U} = \log^{10} \left(\frac{P}{U} - 1 \right) \quad . \qquad (2)$$

It follows that C is negative for $P/U < 1$ and positive for $P/U > 1$. The following discussion considers only the latter case. The right side of Figure 4 can be plotted with this new scale. This is done in Figure 5 where the axis of the abscissa indicates the log of the contrast function and the ordinate gives the log of U in lux. In addition to the curves of Figure 4, the curves for γ = 50, 100, and 200 min are also given. With these data, minimum visibility has been established. The next step is to increase the demands on the observer. The following section will define visibility acuity and sensitivity of the normal human eye.

B. Visibility Acuity and Sensitivity

For measuring visual efficiency, certain test objects, numbers, individual letters, or letter tables are in use, e.g., Snellen hook, block letter charts, Landolt broken circle, and others. The scale for visual acuity is defined as the reciprocal of the diameter of an object which represents the angle at which the shape of the object is just observed. For research purposes the Landolt circle is generally adopted (Figure 6).

In this test it is the task of an observer to find the opening in the circle under the test conditions of interest for different sizes of circles. From the requirements on the observer, the visibility acuity became an angle resolution acuity method. Other acuities, for example, are vernier, stereo, and motion acuities. By international agreement (1909), visual acuity was defined as the reciprocal of the threshold angular substances of the gap in a black Landolt "broken circle" on a white background. It is given directly in Snellen Units, S, when the threshold is expressed in minutes of arc as follows:

S = 1 width of gap (or diameter) = 1 min

S = 0.1 = 10 min

S = 2 = 0.5 min, and so on.

Visual acuity is a form-related definition, and in order for data to be usable and acceptable they must always be obtained on the same test object. This is fulfilled in the cases of the Landolt circle and the circular disk. Again, the data of Observatory Jena are used. Up to this point, the "blackness" of the test object has not been discussed; it will be explained in the following paragraphs.

The totally black surface has an intensity reflectance R = 0, whereas the background, the totally white paper plane, has the reflectance R = 1 for all wavelengths in the visible part of the spectrum. With this condition, the values of visual acuity are optimum ones. In order to meet actual cases, and because all bodies in nature have more or less colored surfaces in which the colors contain more or less black and white, these tests also included grey rings. With respect to the white background, the Landolt circle with a reflectivity of 60% (for all wavelengths) occurs under a contrast C = 0.60. The curves in the illustrations are marked in this sense. In the experiments the Landolt circle was fixed in front of a white background and uniformly illuminated in a certain range of intensities. The illumination is given in lux. The ring, and therefore the position of the gap, is changed form one observation to another; the observer must find the direction of the gap in at least nine out of ten observations. The results of a series of tests are given in Figure 7.

The axis of the abscissa gives the illumination in lux; the axis of the ordinate gives the visual acuity in Snellen units. Each iso-contrast curve divides the plot into two areas. S represents the reciprocal of the angle under which the object occurs for the observer. In the area above the curve it would occur under a smaller angle. It will become visible only if the contrast can be increased. The curve marked with 100% gives the maximum visual acuity for the human eye for the corresponding illuminance, and since R = 1 for the background, for the corresponding luminance of U in apostilb. The maximum value of S itself can be obtained only if the illumination on U is on the order of 30,000 lux, then S = 2.45. This value was also reached in the tests.

As a test object the Landolt circle has a substantial disadvantage; it was found expedient to use the circular disk in the visual acuity test. To understand this critical objection, the area around the gap in the circle should be considered. The quadratic slit, the perceptibility of which is the demand on the observer, abuts upon two sides on the dark ring and on the remaining sides on the background of the same illumination and luminance. This condition produces complicated proportions at the cones and rods of the retina, especially at the smaller angles of view. The circle test turns into an acuity test if a kind of objective examination is employed, in which the observer has to locate the disk wherever it occurs on the background. In order to realize this, the disk was mounted on an eccentric revolvable device. The data thus obtained (Figure 8) are similar to those of the Landolt test, but the maximum of visual acuity is S = 3.75. The curves of Figures 7 and 8 show that with more brightness and greater contrast the acuities S obtained for the circle tests are larger than those obtained in the Landolt test. At lower brightnesses of U and at smaller ratios of contrast, the observer noticed the gap in the circle before he detected the disk itself (Figure 9). This is a surprising result, but it can be understood if the matter is explored further.

These experiments already show how complicated it is to define visibility for the human eye. Figure 10 compares the visual acuity curves for the Landolt and disk tests for the case in which both objects are totally black. On the axis of the abscissa are some notes with respect to the functions of the eye. A Landolt test gave better value for S in the inerval of brightness which occurs just before or after sunset. With decreasing brightness, S also decreased. For the eye there is a transition region where the optical process turns over from the cones to the rods. The curve for the Landolt test shows a remarkable irregularity.

C. Visual Performance

The third step, precise understanding of the object, has not been systematically studied in research work. At the present time only the results of Nagel and Klughardt [5] can be used. In general, test objects similar to those previously mentioned can be employed merely by putting higher demands on the observer. A grey Landolt circle of contrast 1:20.4 placed in front of a white background was used as a test object. The acuity was defined by

$$S = \frac{s}{dy} \tag{3}$$

where s is the distance in which the object of diameter dy (in this case the outer diameter of the circle) is just perceptible. The values obtained were lower than in the other tests and were plotted in Figure 11 with other available data, some of which were not discussed here.

D. Visibility of Light Sources

In Section II A, the visibility of a circular disk was discussed and the data presented in Figure 5. In this method the fields U and P were projected on a screen. The field P can be considered as a light source of area extension. In general, anything which can be seen by the eye is only visible because it emits radiation into the eye. Whether the radiation is from a primary or secondary light source is of no significance to the eye. In other words, the disk test represents light sources of certain extension. Therefore, the data of Figure 5 can be used for actual light sources, which are placed a certain distance away, 100 m. As an example, it is assumed that such a light source appears under an angle of 1 min and that the luminance of the background is 10^{-2} stilb. From Figure 5, $\sigma = -0.46$, and the following is obtained:

$$\sigma = \log (P - U) - \log U = -0.46$$

$$\log U = \log 10^{-2} = -2$$

$$\log (P-U) = -0.46 - 2 = -2.46 = 0.54 - 3$$

$$P = 1.35 \times 10^{-3} \text{ stilb.} \qquad (4)$$

The area P, seen under an angle 1 min of arc, has a diameter of 2.91 cm and therefore an area of 6.6 cm^2. The luminous intensity in candles (HK) then becomes: $6.6 \times 1.35 \times 10^{-2}$ stilb = 0.089 HK. Light sources are generally more applicable during the dawn and at night. If they are not of too great an intensity, they appear like stars. The fixed stars are only bright gas spheres which are so far away that they appear as point sources even under high magnification. Their apparent size is expressed in stellar magnitudes, that is, the visual brightness as seen from earth. The observer becomes independent of the 100-m distance if the astronomical magnitudes are accepted. One HK at a 100-m distance is equivalent to the luminous intensity of a star of $-4.^m0$. The following is obtained:

$$0.089 \text{ HK}: \quad -1.05 \times 2.5 = 2.^m625$$

$$P: \quad -4 + 2.625 = -1.^m4. \qquad (5)$$

In this sense, Figure 5 was transformed into Figure 12, which illustrates the visibility of light sources as a function of background brightness, of vision angle, and of luminous intensity, first in HK (left side ordinate) and then in stellar magnitudes (right side ordinate). The human eye can see stars down to a stellar magnitude of approximately $+6.^m0$. The entire test used a white paper screen as a background, which was uniformly illuminated. The next section will discuss the brightness of sky and terrain, which in practice are the backgrounds of objects.

III. BRIGHTNESS AND ILLUMINANCE OF SKY AND TERRAIN

A. General

The brightness of object and background depend on their position with respect to the sun and on their reflection properties. The intensities of the radiation which reach a given point on the earth's surface vary in an interval of approximately 90 dB. The spectral intensity distribution also follows a daily course.

To illustrate the illumination by the sun a white plane of paper is placed parallel to the earth's ground (Figure 13). The test field receives both direct sunlight and diffuse light from the whole sky. It is easily understood that the intensity of the light received directly from the sun is proportional to the cosine of the sun's height h . and that it depends on the attenuation which the light suffers during the path through the atmosphere. The diffuse component of the received radiation originates in a far more complicated manner. Multiple scattering occurs in the atmosphere among many kinds of particles — atoms, molecules, dust particles, water droplets, etc. Each particle becomes a scattering center and emits light of different power in all directions, including the direction of the test plane on the ground. After sunset no direct light reaches the test plane; the last diffuse sunlight is received there when the sun is 18.5° under the horizon for that specific point.

The individual regions of the sky differ in brightness and change with progressing time. The brightness of sky and terrain are determined by the same geophysical, astronomical, and meteorological parameters. The elements affecting the brightness of the terrain or of an air element are as follows:

1) Position of object of consideration.

2) Position of the sun (azimuth, altitude, time, and declination).

3) Geophysical and meteorological elements (mattter, atom, molecule, shape and kind of small particles, dust particles, water droplets, clouds, rain, fog, etc.).

4) Weather elements close to the ground.

5) Shape and reflectivity of object (color, roughness, inclination towards ground, etc.).

All of these factors could be considered in a mathematical determination of the brightness of sky or terrain; however, more useful data can be obtained more rapidly by experimental methods.

B. Experimental Determination of Brightness and Illuminance

In experiments a photoelectric cell (Figure 14a) is placed parallel to the earth's surface and voltage or current produced by the radiation is measured. The intensity contribution of special spectral regions can be measured by using filters. In order to measure the brightness of a specific area of the sky, that region can be imaged on the surface of the detector. With such methods, for example, the brightness on the unit per square degree was measured. Data on the sky's brightness close to the horizon are of particular interest here. Theoretically, any region of the sky can be controlled for any time interval wanted; such a program would contain a great number of specific cases, and the data would be of great value.

As an example, the general case of the flat plane parallel to the earth's surface is considered. Some of the results received from approximately 250 different experiments [6, 7] are examined. These experiments used measurements by photoelectric (65 days) and visual photometric (182 days) methods (Figure 14b). These results are from a selection of the most usable data obtained on more than 300 days. In the photoelectric method, detectors with different filter combinations were used. The measured data were noted in time intervals up to 30 sec. All data must be reduced to the true time or true high of the sun. The latter depends on the time (τ), sun's declination (δ), and geographic latitude (φ), and can be obtained from the following:

$$\sin h_{\odot} = \sin \delta \sin \varphi + \cos \delta \cos \varphi \cos \tau \quad . \tag{6}$$

Three plots (Figures 15, 16, and 17) illustrate the change of the sun's height during a day for the sun's declinations $\delta = +23.5°$, $0°$, and $-23.5°$. Figure 15 is for the latitude $\varphi = 55°$, where the following measurements were made. Figure 16 is for $\varphi = 40°$, which corresponds to Madrid, New York, Chicago, and Korea. Figure 17 with $\varphi = 60°$ corresponds to Oslo, South Alaska, and Leningrad.

The spectral efficiency of the photocells was adapted to match that of the human eye by special filters. Other filters were used to obtain the color index. From these data the color temperature of the sky can be calculated. In the visual method, a visual photometer was used; thus the brightness of a white plane illuminated by the whole sky was compared with another bright plane in the photometer until equality in brightness of both fields was obtained. The effect on the illumination of meteorological elements, particularly cloudiness, was also of interest; therefore, the final results were arranged in groups on the basis of cloud conditions. The illumination of the sky is given in candles which converts directly to the brightness value in lux; 1 HK is equivalent to 0.92 standard candlelas. Figure 18 is an illustration of the brightness course during a day for the horizontal plane.

The axis of the abscissa marks the height of the sun over or under the horizon. At sunset, $h_{\odot} = 0°$; negative heights occur after sunset. The axis of the ordinate shows the brightness in lux. Because of the enormous change in brightness during one day — from approximately 100,000 lux at noon to approximately 0.0003 lux at night — the axis of the ordinate is given in a logarithnic scale. The plot contains three main curves. Curve 1 is the average value of brightness of days with clear sky up to a 5/10 cloud-covered sky. The heaviest change in brightness occurs between $h_{\odot} = -5°$ and $h_{\odot} = -15°$. It is night when the sun's depression becomes $h_{\odot} = -18°$. This called the end of the astronomical dawn. If there is no meteorological change, the brightness will stay constant throughout the night until the sun again reaches $h_{\odot} = -18°$; then the brightness will follow the curve in the opposite direction of the axis of the abscissa, toward increasing brightness, etc. There is no difference between the brightness change from day to

night and that from night to day. Curve 2 of Figure 18 illustrates the lowest measured values of brightness. These data were obtained on a "dark day" with 10/10 cloud-covered sky. On such a day, night begins when $h_\odot = -16°$. The portions of the curves depicting higher sun elevation are based on a smaller number of experimental data, because the main interest was to measure the brightness change from approximately one hour before sunset until night. This had not been done prior to this study. Weather changes constantly; it is nearly impossible to get a complete curve for the lowest brightness during a day. Before rain starts, it sometimes becomes quite dark. Physiologically it is felt that the decrease in brightness is very great when, in fact, the decrease in brightness is generally only down 0.2 or 0.1 from the value before. Because the experimental devices were not designed to measure during rain, precise statements cannot be made as to how far the brightness goes down in the case of rain. Another curve in Figure 18, Curve 3, presents the highest measured brightness ever achieved in this test.

C. The Brightness Change on a Specific Day and Point on Earth

The axis of the abscissa, true height of the sun, of Figure 18 relates the data of brightness to any day in the year. Assuming that the maximum height of the sun is $h_\odot = 50°$, for these data, the following relation can be used:

$$h_{\odot\,max} = 90° - \varphi + \delta \quad , \tag{7}$$

where φ is the geographic latitude and δ is the sun's declination for that specific day. The point of consideration may be located at $\varphi = +50°$, and $\delta = +10°$ is obtained. The sun has any given declination twice a year; from astronomical almanacs the declination is found to be $\delta = +10°$ on approximately 27 or 28 August and 16 or 17 April. The distance the sun goes under the horizon on the previously mentioned days must be checked in order to find the lowest brightness. It is of importance to find that the sun really reaches the height $h_\odot = -18°$. If this did not happen, "midnight dawn" would occur. The condition that any given point on earth reaches the end of dawn can be expressed as

$$\varphi + \delta \geq 90° - 18° = 72° \quad . \tag{8}$$

In this example, $\varphi + \delta = 50° + 10° = 60°$, which is smaller than 72°; that is, the sun actually sets not just 18° under the horizon but goes down to $h_\odot = -30°$. Therefore, Figure 18 illustrates the entire course of the brightness for the mentioned four days. The curve for the lowest brightness could be extended in a straight line to $h_\odot = -30°$ which the sun reaches at midnight.

It is noted that this curve illustrates the change in brightness during a day for all points on earth which are located at the geographic latitude $\varphi = +50°$.

This material, which shows the average of the change in brightness with the height of the sun, is applicable to all geographical latitudes. Although the critical reader may argue against this, there are not sufficient experimental data available on other latitudes to provide for any other approach. The brightness values are obtained from Figure 18. These data are plotted on Figures 19 and 20 for the geographic latitudes $\varphi = 40°$ and $\varphi = 60°$. Figure 19 gives the brightness for Madrid, New York, Chicago, and Korea; Figure 20 gives the brightness for Oslo, South Alaska, the middle of the Bering Sea, Hudson Bay, and Leningrad. Figure 20 shows that in winter in Oslo ($\delta = -23°$) there is a dawn of nearly three hours; it never becomes night during that season. These results present information about the total brightness. For experiments with detectors which measure only in certain wavelength intervals, it is of interest to know more about the spectral distribution of the luminous flux which is received on the earth's surface.

D. The Color of Skylight

It is assumed that the spectral energy distribution of the light received on earth resembles the distribution of a black body. It is further assumed that the light, which is changed by the previously mentioned scattering process, always follows Planck's law. Experiments are conducted with only those instruments whose spectral response is well known from scale measurements. It is advantageous to use filters which select individual parts of the radiation spectrum from the two edges of the response of the employed detectors. For this reason, a red and a blue filter were chosen. The spectral responses of the receivers and filters used in the reference test are plotted in Figure 21. The color index is defined by the logarithm of the ratio of the radiation in the red region to that in the blue region of the spectrum. In this case the color index becomes

$$C = F.I. = \lg \cdot \frac{\text{Voltage of Red Part of Spectrum}}{\text{Voltage of Blue Part of Spectrum}} \tag{9}$$

The arbitrariness of this method can be avoided if color temperatures are used. It would be more exact if this temperature is called the "color index temperature." The color temperature for each specific experimental datum follows from:

$$C = F.I. = \frac{\int_0^\infty E(\lambda,T) \cdot e(\lambda) \cdot \phi_r(\lambda) d\lambda}{\int_0^\infty E(\lambda,T) \cdot e(\lambda) \cdot \phi_b(\lambda) d\lambda} \tag{10}$$

where

$e(\lambda)$ = the spectral sensitiveness of the detector,

Φ_r and Φ_b = the transparencies of the filters,

and

$$E(\lambda,T) = \frac{c_1}{\lambda^5} (e^{c_2/T} - 1)^{-1} \quad . \tag{11}$$

The preceding equation is Planck's function of the energy distribution in the spectrum of a black body with the constants c_1 and c_2, which are given by

$$c_1 = 0.589.10^{-12} \text{ W cm}^2$$

$$c_2 = 1.432 \text{ cm deg.} \tag{12}$$

By means of these equations and by graphical integration, the measured F.I. values are transferred into c_2/T values. The relation between color index and color index temperature is illustrated in Figure 22. Figure 23 illustrates, for one day, the following:

1) The brightness course of the visual region of the spectrum.
2) The red region received with the red filter combination.
3) The blue region received with the blue filter combination.
4) The F. I. curve reduced from these experimental data.

The color of the sky, as already mentioned, depends also on weather conditions. This is illustrated in Figure 24. The axis of the abscissa denotes the height of the sun; the left axis of the ordinate, the values $c_2/T.10^{-4}$; and the right axis of the ordinate, the absolute temperature which corresponds to the color distribution. During the day when direct sunlight is received, the radiation of the sun dominates the scattered light and even clouds are not too effective, because the strong forward scattering of very small water droplets contributes to the intensities received directly from the sun. During dawn the color changes from red to blue and has its intensity maximum at the shorter wavelenghts when the sun is approximately 10° under the horizon. Toward night the color temperature goes down at the end of the twilight, it reaches approximately 4200°K, a temperature which is lower than that during the day. The human eye is not able to detect this last fact, because at night it distinguishes only between black and white. The eye can observe only a change in energy, and can determine, for instance, only that it is now darker than it was a short time before.

It follows from Wien's law

$$\lambda_{max} \cdot T = 0.288 \text{ cm deg}, \qquad (13)$$

that the maximum of radiation occurs for

6000°K	at	4800 A°	day
15,000°K	at	1920 A°	$h_\odot \sim -10°$
30,000°K	at	960 A°	T_{max}
4200°K	at	6800 A°	night sky

Sections B and C and the first part of this section considered radiation received from the whole sky, which is also called the global illuminace. The brightness of the zenith will now be discussed.

Astronomical measurements were undertaken by W. Brunner [8] in 1931 and 1932 with a visual photometer proposed by Dufay. His measurements covered the range from +60° to -17° $_\odot$, but only the data from +1° to -17° $_\odot$ are available. The results of the average brightness of the zenith, measured in stellar magnitudes, are represented in Figure 25.

Another set of experimental data obtained by K. Bullrich [9] covers the range from 20° to -15° $_\odot$ (Figure 26). It is noted that the axis of the ordinate is given in apostilb (asb), because the luminance of the zenith region is being sought. The clouds now have the effect of increasing the luminance and the clear sky shows a lower brightness.

It is fortunate that illumination on earth is not confined to direct sunlight. The brightness or luminosity of the sky during the day has been given considerable study in illuminating engineering. From the studies of H. H. Kimball [10], for example, several publications are available which show contour lines of constant luminosity an a function of azimuth Φ from the sun and of altitude $h_\odot$. Generally, the luminosity of the sky without clouds or with only light clouds (Ci, Cs) is greatest near the sun and reaches a minimum approximately 90° from the sun. With dense clouds, the luminosity is practically independent of Φ, but is a function of $h_\odot$, having a maximum value at the zenith irrespective of the position of the sun. Evidently the luminosity of the sky is far from uniform. The shape of the luminosity distribution curves shifts with the position of the sun and with the condition of the sky.

On the basis of the facts given, it follows that for a cloudy sky the illumination of a vertical surface is almost independent of the orientation of the surface. With a clear sky, the illumination is much greater when the surface faces the sun and reaches a minimum value when the surface is turned through 180°.

IV. THE VARIATION OF THE VISIBILITY DURING A DAY

The background luminance in the tests covers the general range of luminance during one day. It is now possible to relate the data of the visibility tests (Section II) to the data of brightness during a day, given for the sun's height or for the true time. The data of Reference 7 are used. The visual acuity for the circle test is illustrated in Figure 27. The decrease in acuity on a clear day starts approximately one hour before sunset and becomes more marked after sunset. At the time when the sun's height is -6°, the acuity is already down to half of its maximum value. At $h_\odot = -9°$, the acuity is only 1/10; after that it changes more slowly until at night it reaches values of only 1/30 of the acuity during the day.

The considerations of acuity in the test are not directly applicable to those data received in operation in open terrain. There is a relatively high contrast in research tests (black test object on white background). In terrain, the contrast in general, is very small. Furthermore, the brightness in the open field, which determines the adaption of the eye and therefore the acuity, is determined also by the average reflectance of the landscape. An average reflectance of 10% is assumed; therefore, the brightness in apostilb is 1/10 the illuminance in lux. Figure 28 is based on this assumption. Each curve divides the plots of contrast and brightness (here expressed by the sun's height) into two parts: one representing the area in which the object is visible for that specific angle of view (left side, above); the other, the area in which it becomes invisible to the observer's eye.

Given the data on brightness and visual acuity of the eye, the variation of view with the horizon as background can be described. From the theory of visibility, the following relation is known for a dark object:

$$S = \frac{1}{a} \ln \frac{1}{\epsilon} \tag{14}$$

where a is the average absorption coefficient and ϵ the relative contrast threshold $\left(\frac{U-P}{U}\right)$ of the eye. The latter depends on the angle of view and on the brightness of adaption. If S_o is the maximal visual distance for optimal $\epsilon = \epsilon_o$ (brightness during the day, angle of view >2°), the following is obtained:

$$S_o = \frac{1}{a} \ln \frac{1}{\epsilon_o} \quad . \tag{15}$$

The visual distance during the time of decreased brightness (dawn, night) is related to those distances observed during the day (S_o), and the following is obtained:

$$S/S_o = \frac{\ln 1/\epsilon}{\ln 1/\epsilon_o} = \frac{\log 1/\epsilon}{2.25} \quad . \tag{16}$$

During the dawn, the brightness of the horizon depends largely on the azimuth; therefore, an average value must be employed for the brightness. The observed data of illumination are read at 6/10 to 9/10 in apostilb instead of in lux. Figure 29 presents the data obtained for the visual distance of objects placed toward the horizon which appear under various angles of view. The illustration shows again the importance of the angle of view. Large objects, such as the tops of mountains and groups of trees, are visible all through the dawn and in the night sky, whereas smaller objects (telegraph poles) become invisible at sun heights -10° to -12°. Only objects whose angle of view exceeds 2° are visible at night.

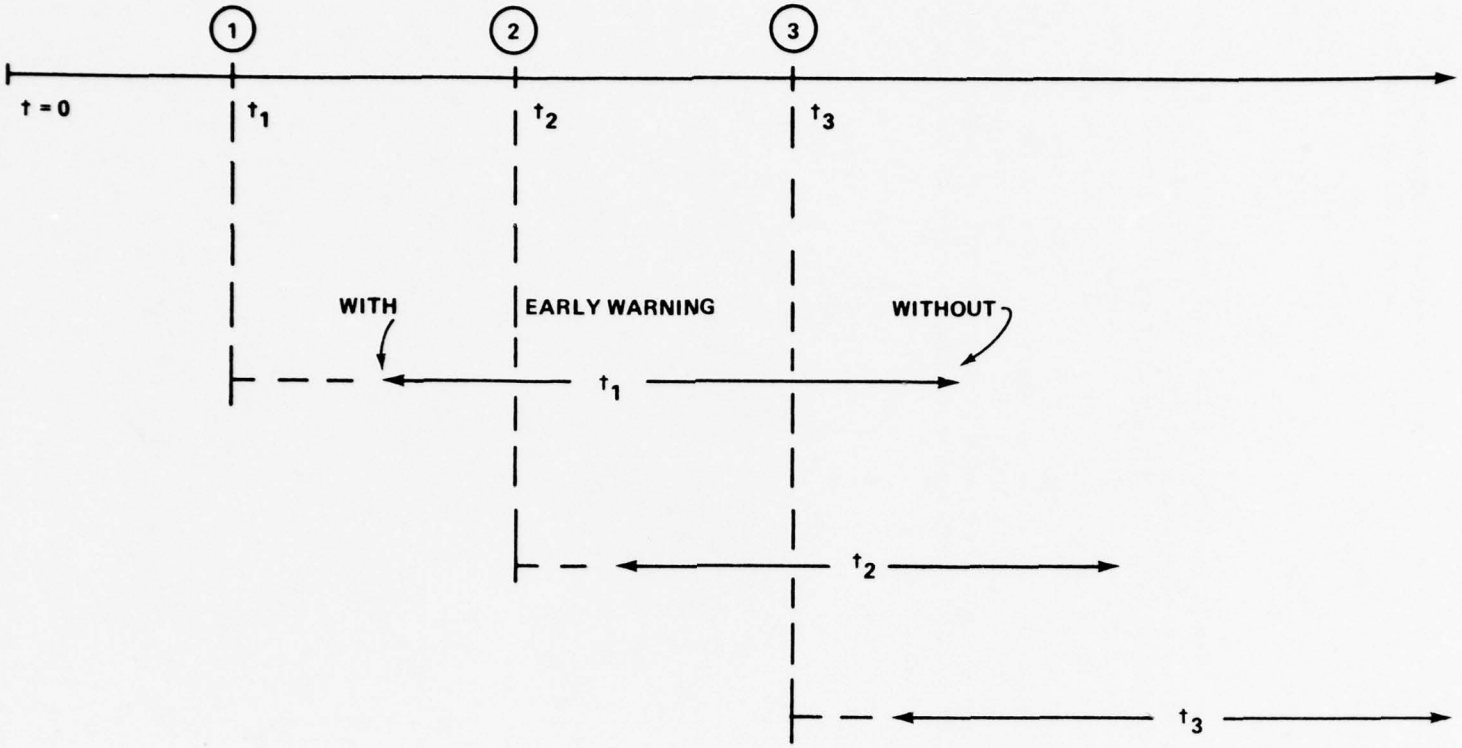

CASE: AN AIR TARGET IS APPROACHING AN OBSERVER.
UPPER CASE: OBSERVER HAS THE INFORMATION THAT A TARGET IS APPROACHING IN A WELL DEFINED PATH.
LOWER CASE: OBSERVER IS RESPONSIBLE FOR A BROADER ANGULAR SECTOR (WITH OR WITHOUT EARLY WARNING).

Figure 1. Visibility and time.

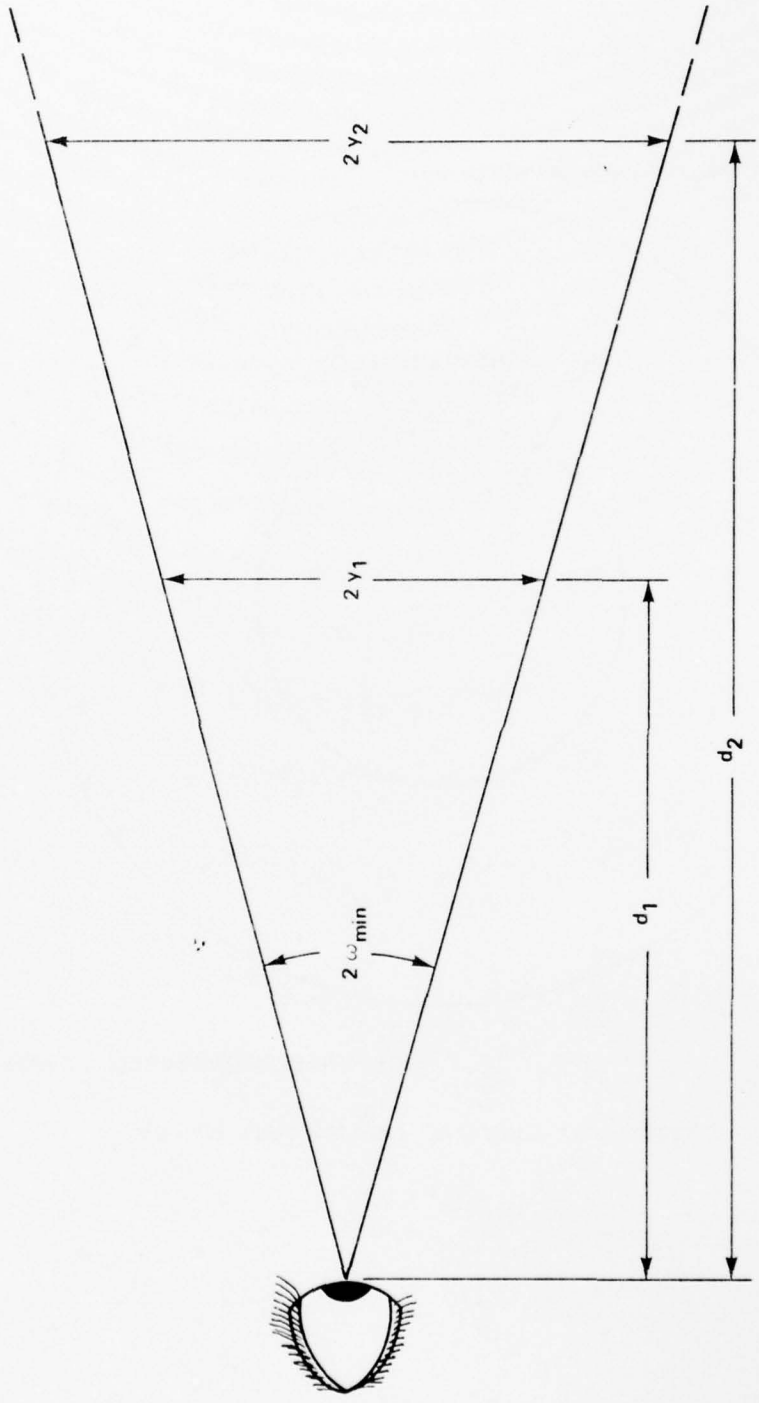

Figure 2. Minimum angle for visibility.

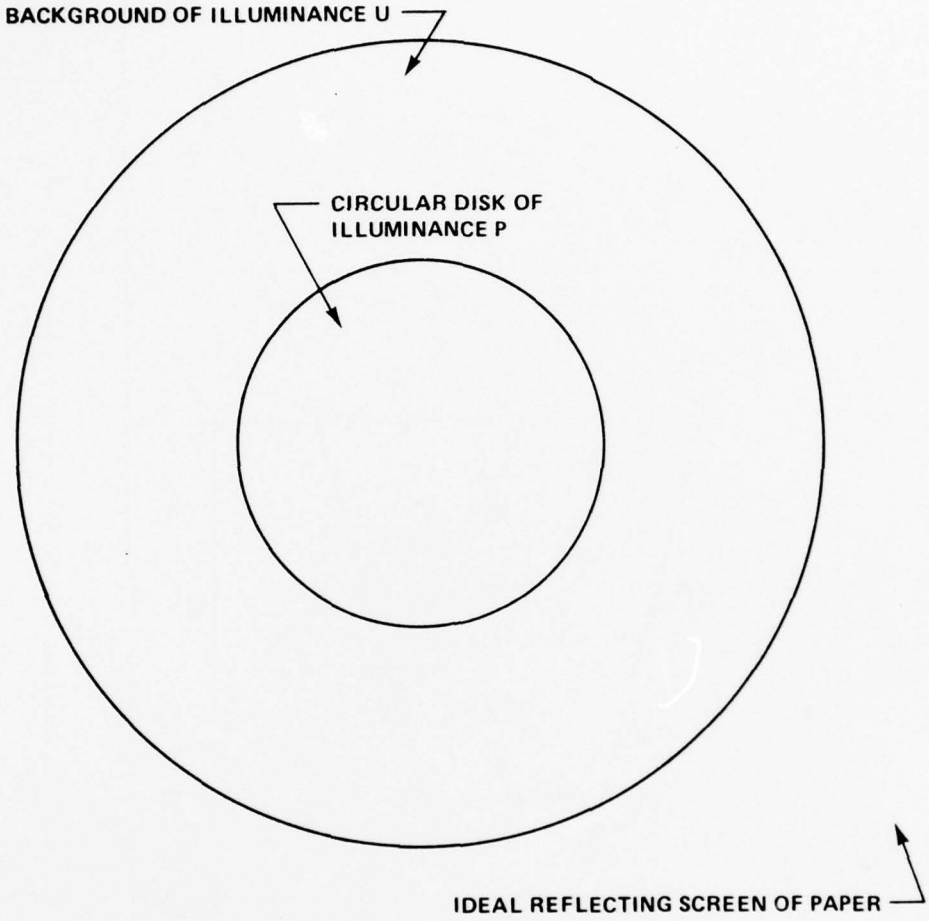

Figure 3. Circular disk as test object.

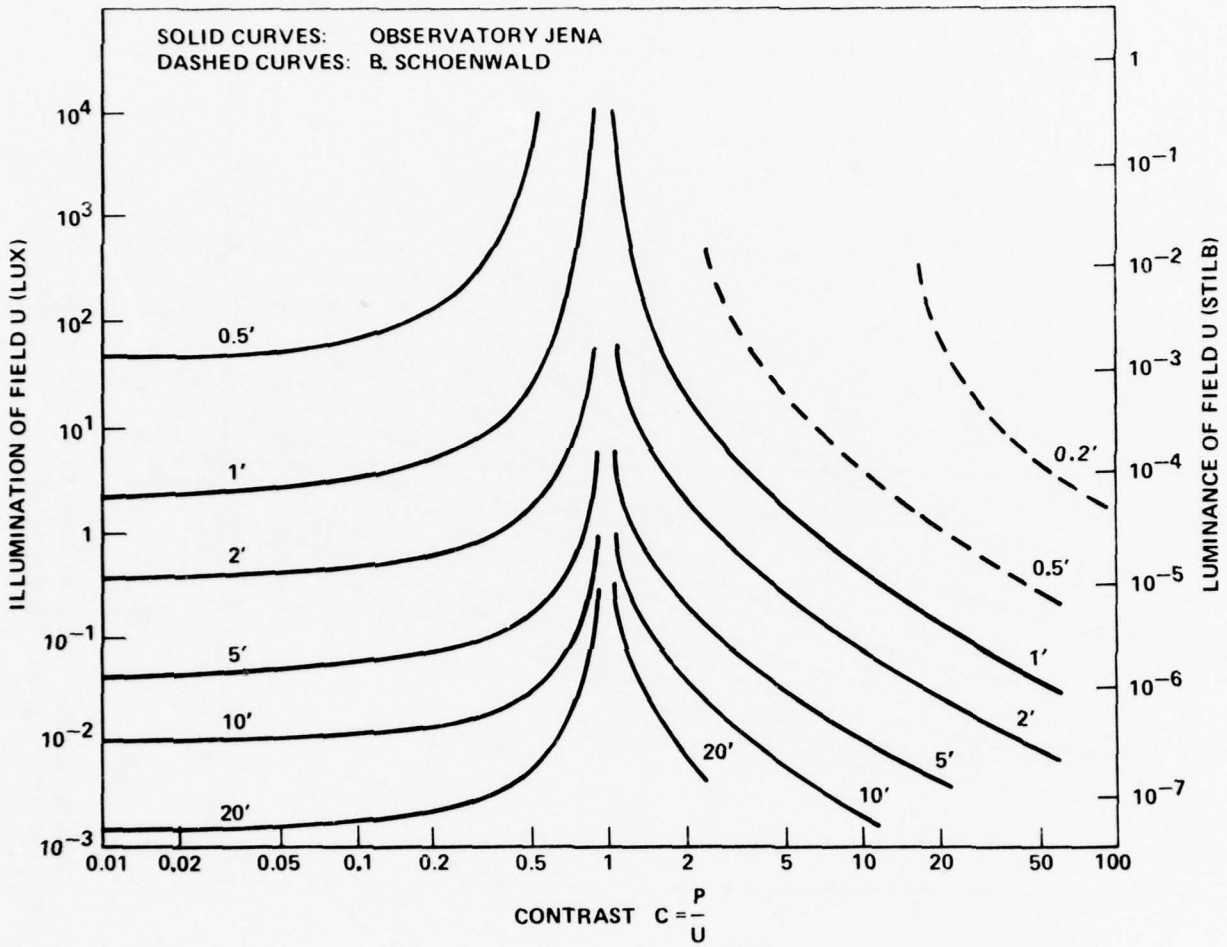

Figure 4. Visibility thresholds of circular objects as a function of contrast, luminance, and angle of view.

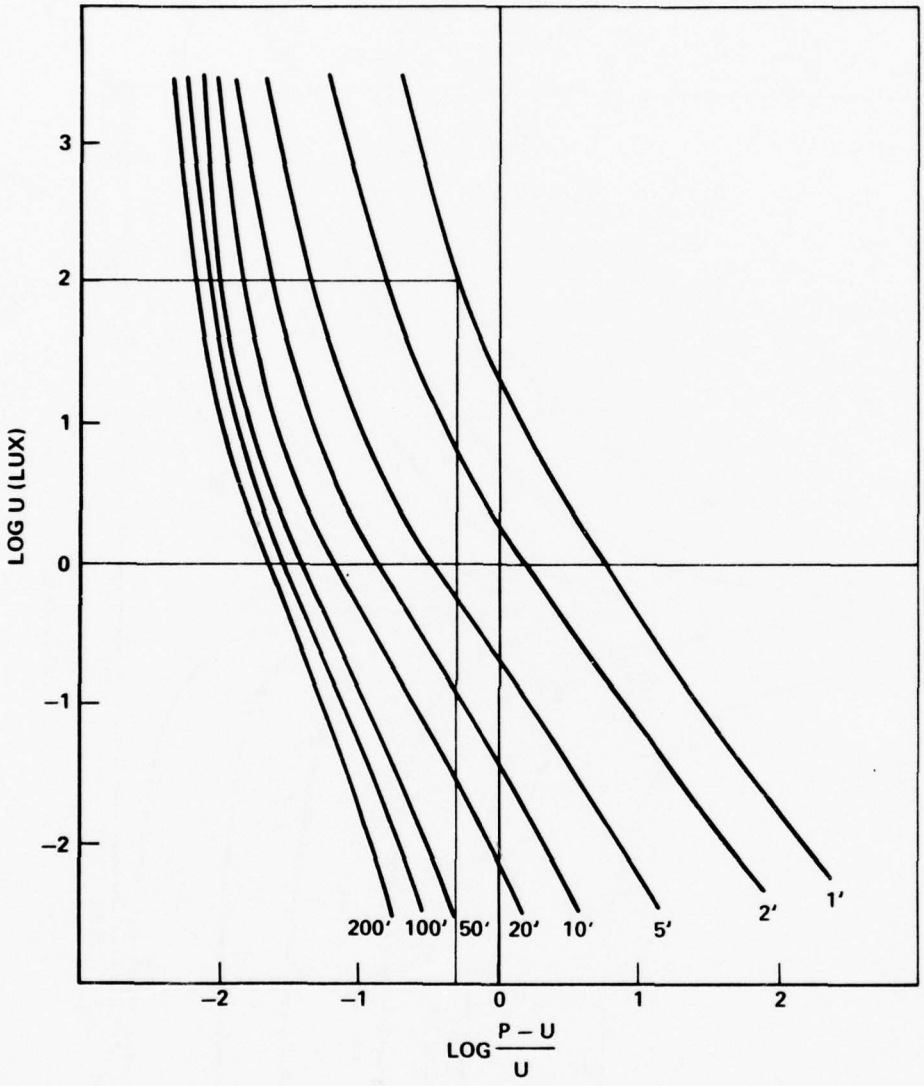

Figure 5. Contrast thresholds as functions of luminance of field U and diameter of field P (circular disk).

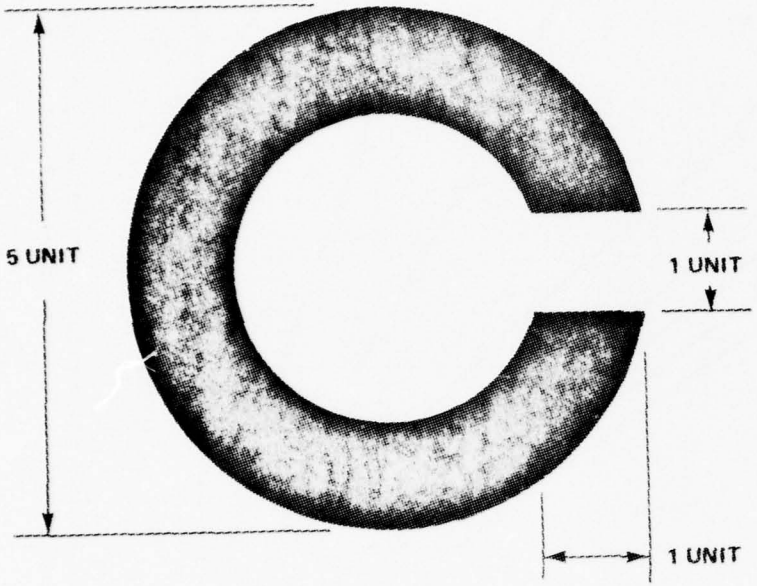

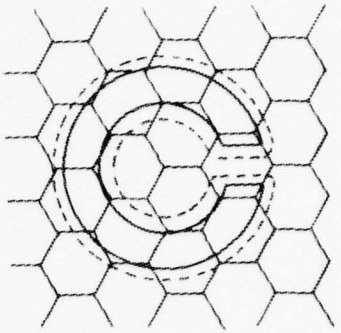

LANDOLT CIRCLE

Figure 6. Landolt circle.

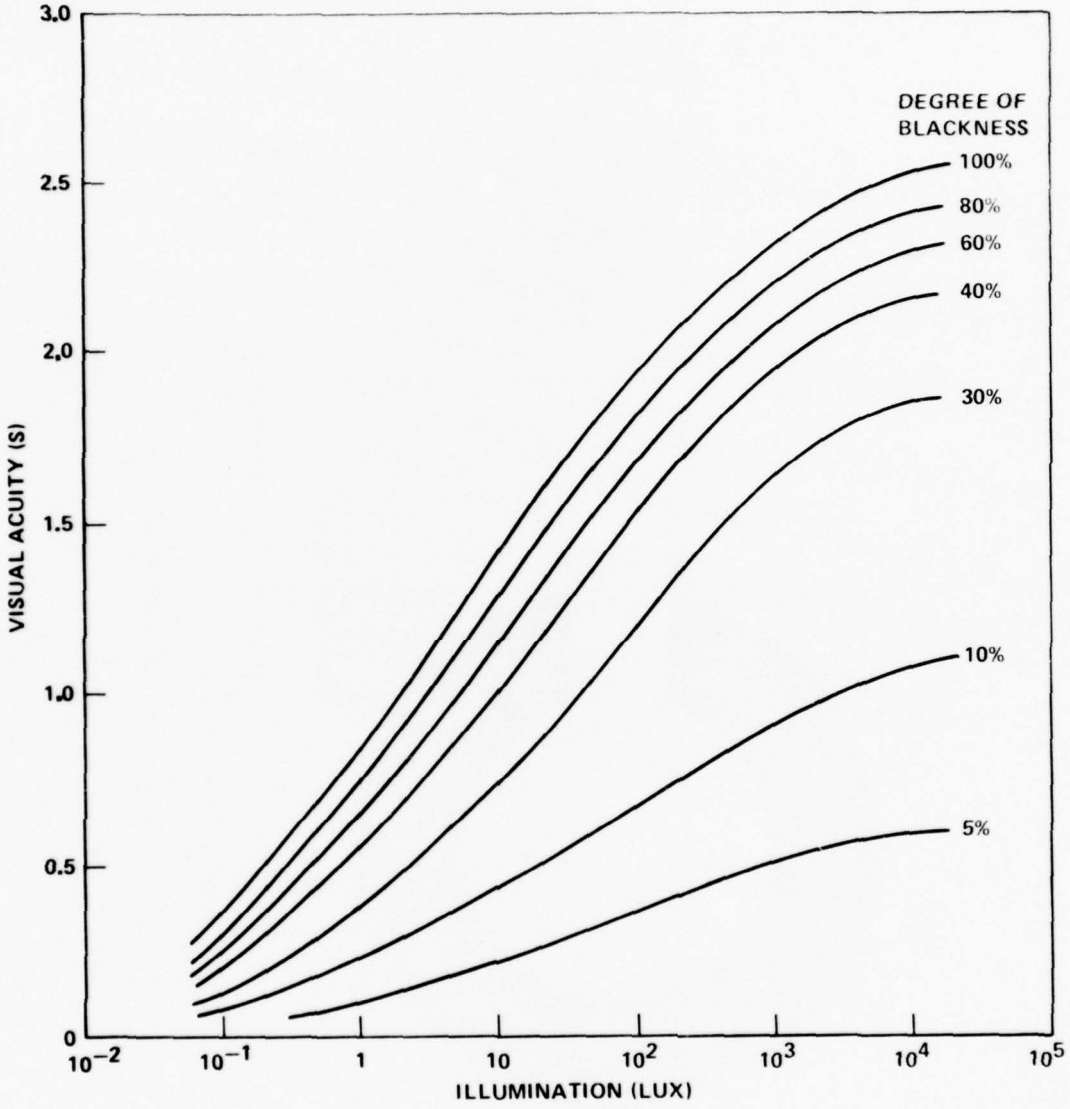

Figure 7. Visual acuity for Landolt circle as functions of illumination and contrast (degree of blackness).

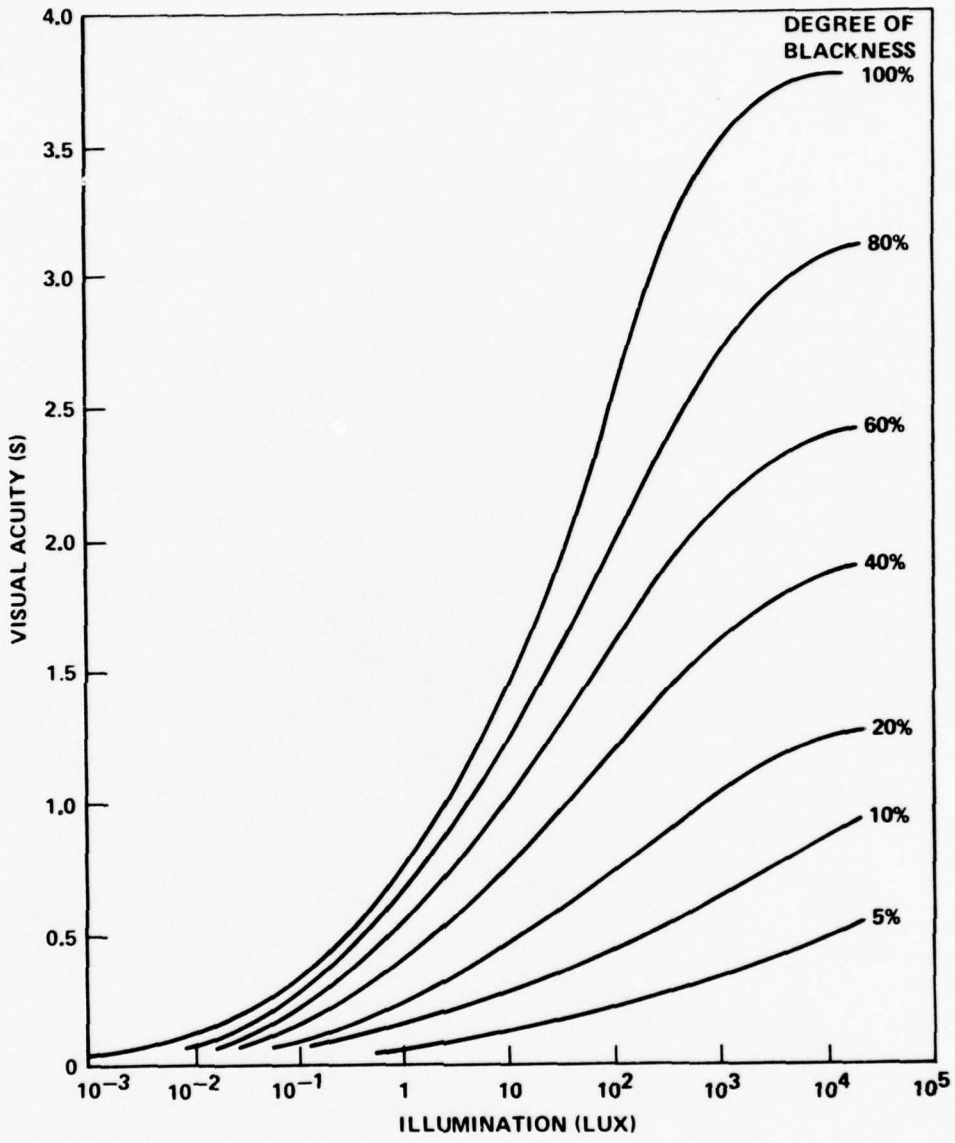

Figure 8. Visual acuity for circular disk as a function of illumination and contrast (degree of blackness).

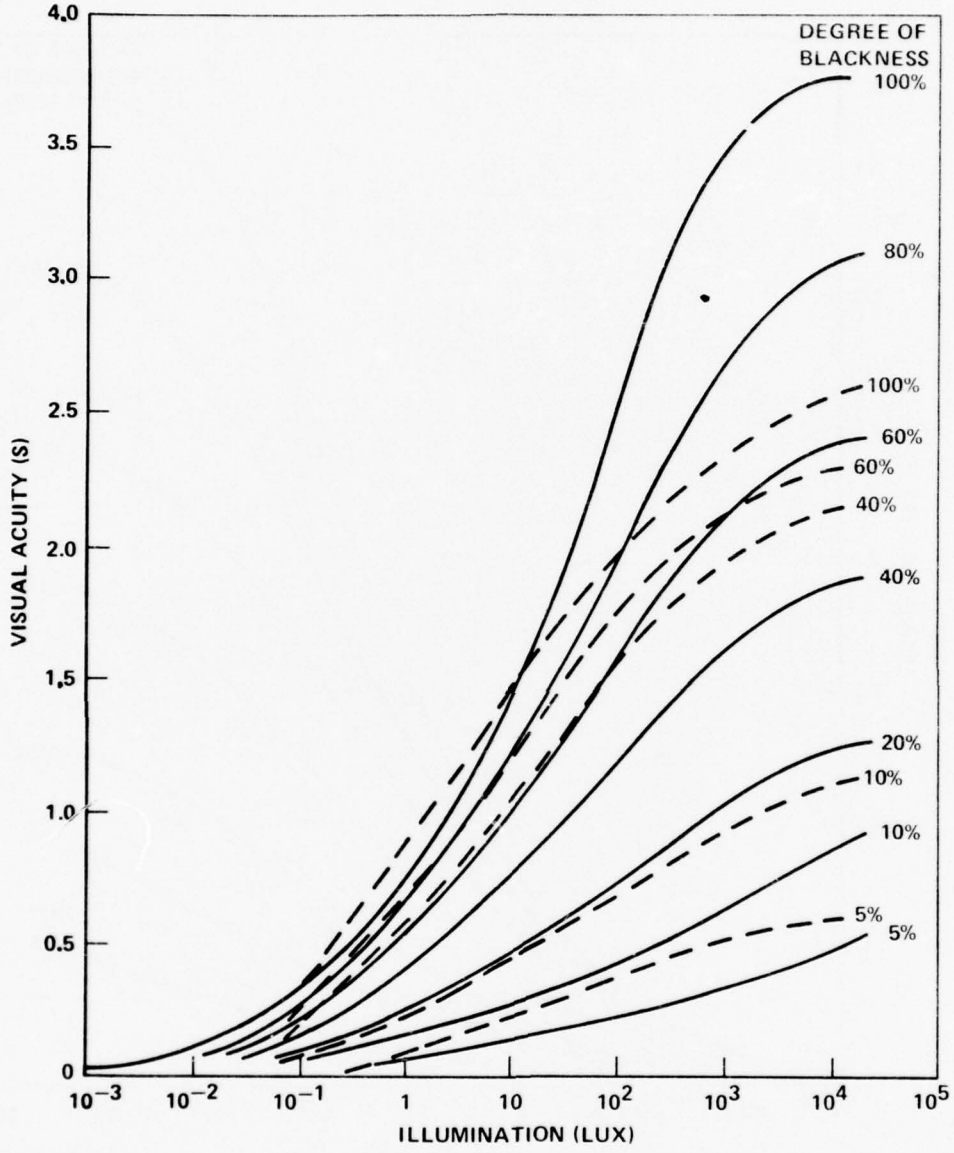

Figure 9. Visual acuity for circular disk (solid line) and Landolt circle (broken line) as a function of illumination and contrast (degree of blackness).

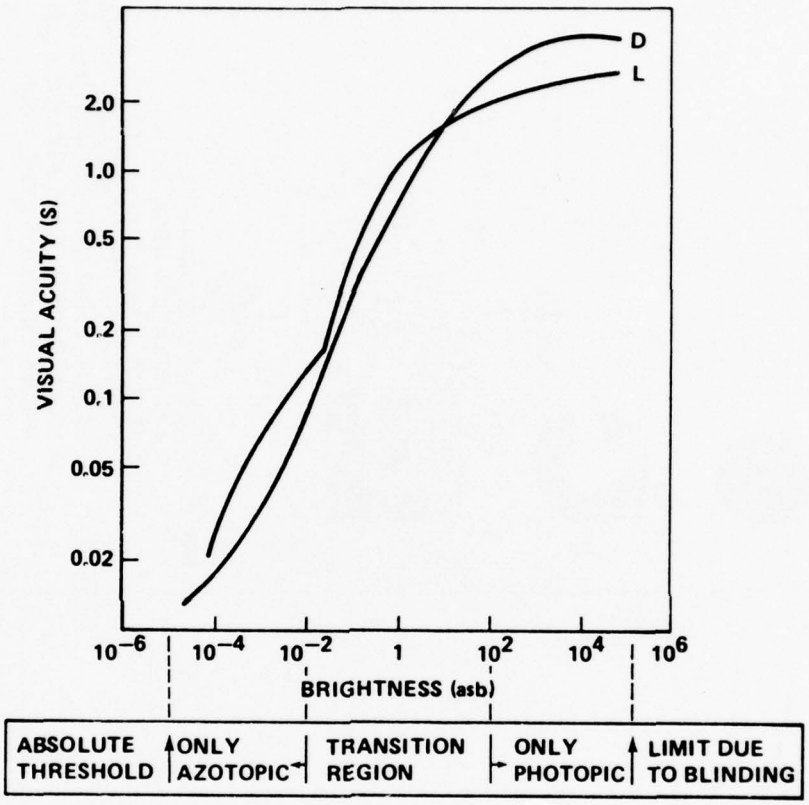

Figure 10. Visual acuity for black circular disk (D) and for Landolt circle (L).

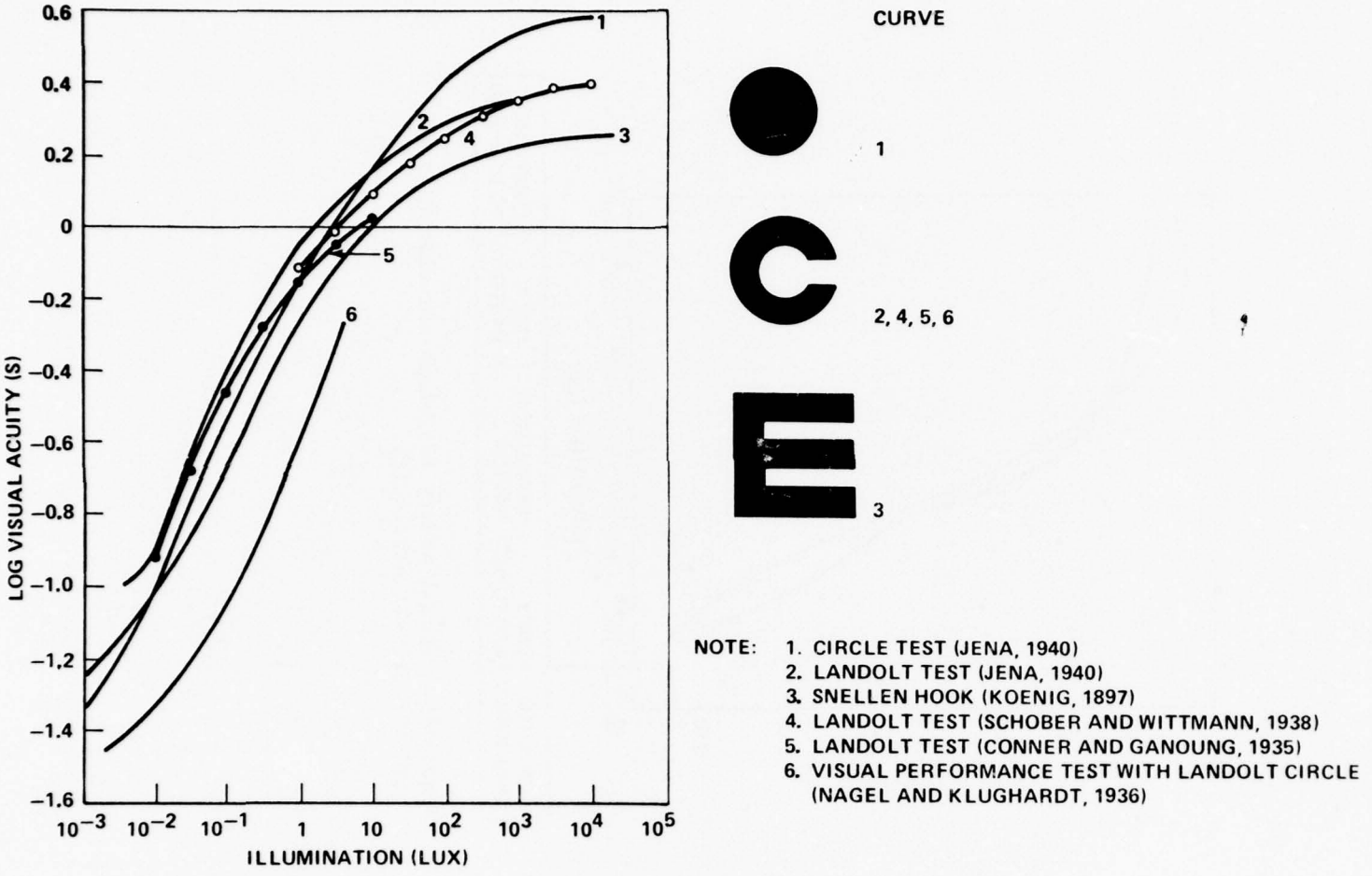

Figure 11. Comparison of different visual acuity tests.

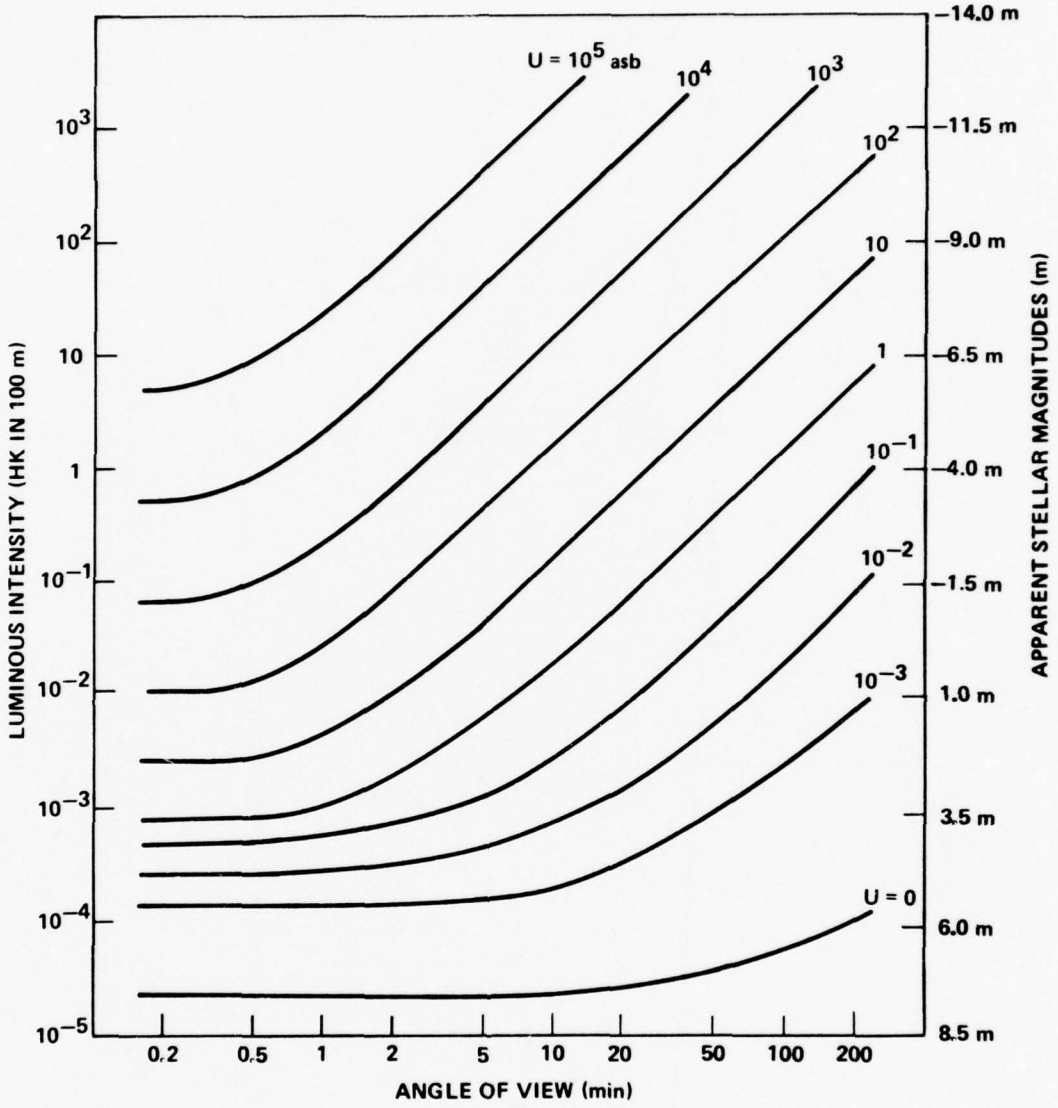

Figure 12. Perceptibility of light sources as a function of background brightness (U) and angle of view.

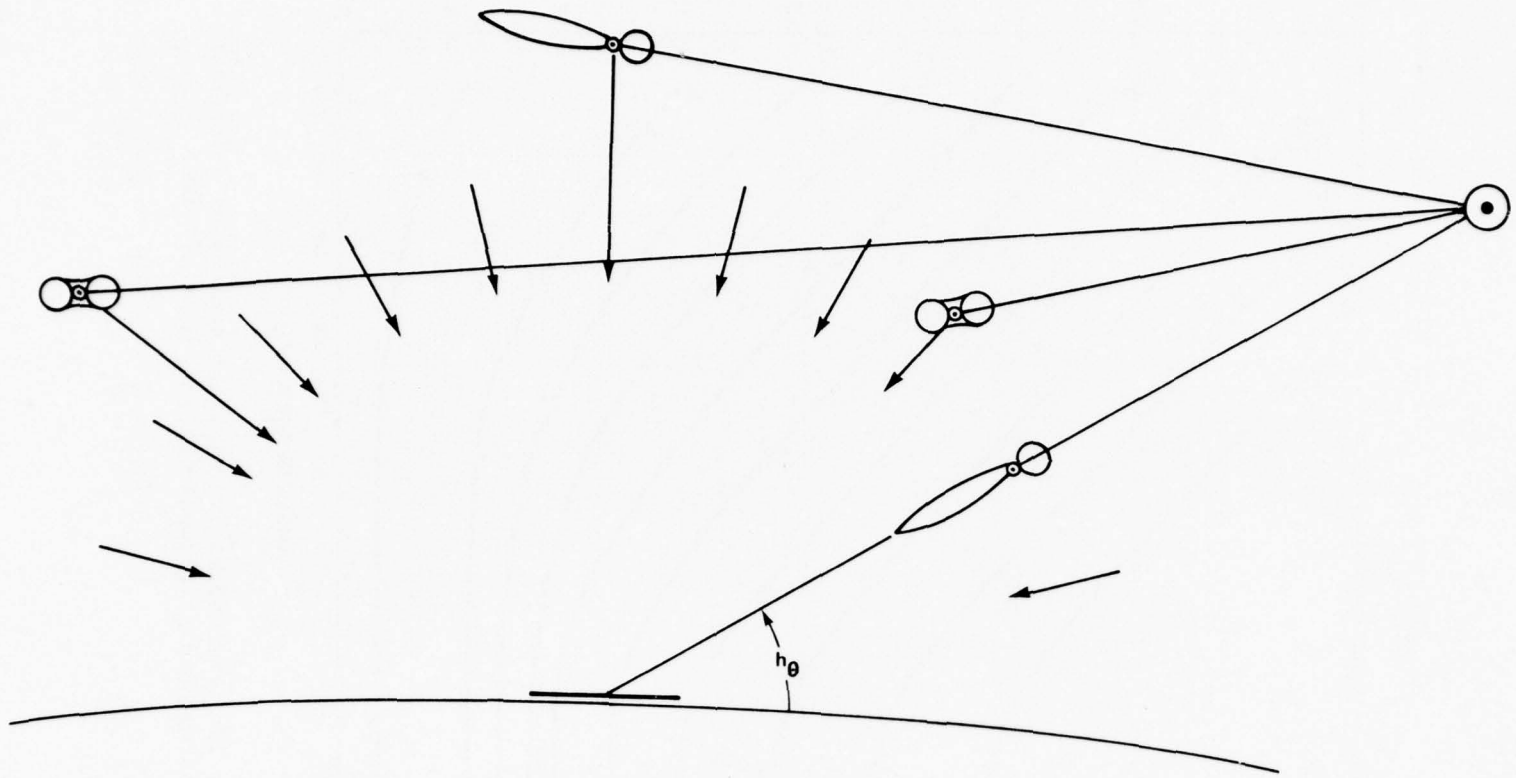

Figure 13. Illumination of a flat horizontal plane on Earth's surface by sun and sky (global illumination).

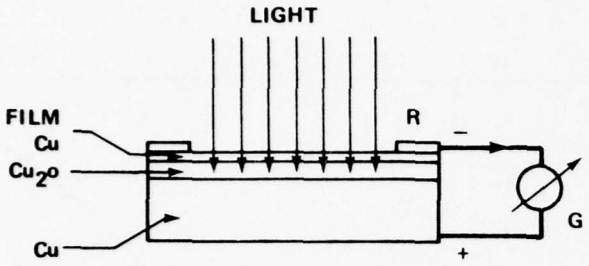

PHOTOELECTRIC CELL
(a)

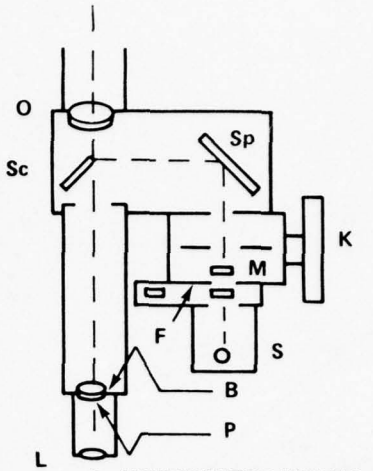

PHOTOMETER VISUAL
(b)

NOTES:

S	SOURCE (4 V, 0.3 A)
F	FILTER – NEUTRAL AND BG 7
M	GROUND GLASS TEMPAX
SC	SCREEN MAGNESIUMOXIDE
SP	MIRROR
K	CAT'S EYE DIAPHRAGM SQ 1 TO 1000 INTERVAL

MAG 3.5
FIELD OF VIEW 15^{o}
MEASURING RANGE
3 3×10^{-5} abs

O	OBJECTIVE, ACHROMAT F = 13 cw
P	EXIT PUPIL 7 mm ϕ

ANGLE INTERVAL 3^{o}

B	LENS +.
L	OCULAR 6x

Figure 14. Photoelectric cell (a) and photometer (b).

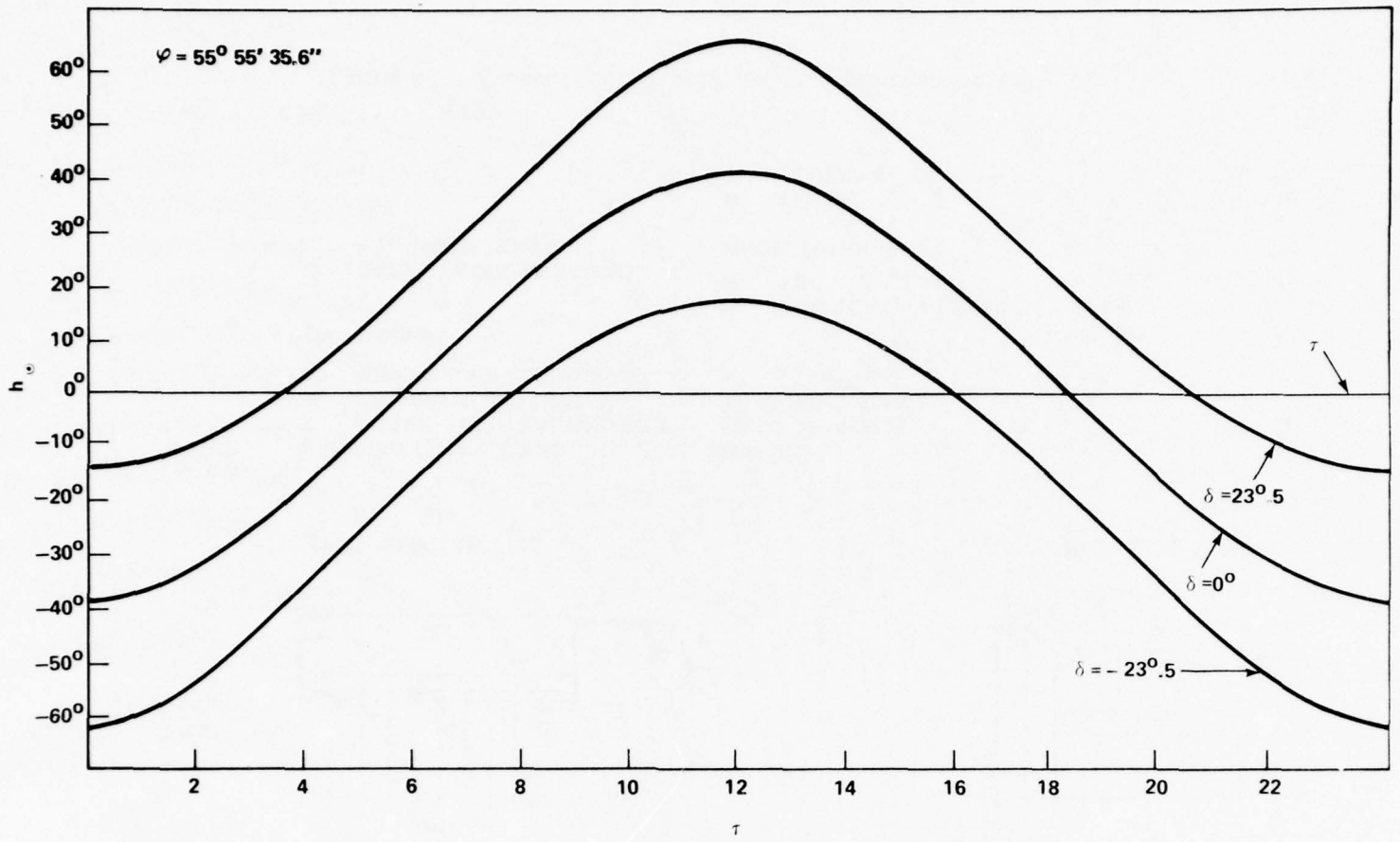

Figure 15. Change of the sun's height during a day (latitude $\varphi = 55°$).

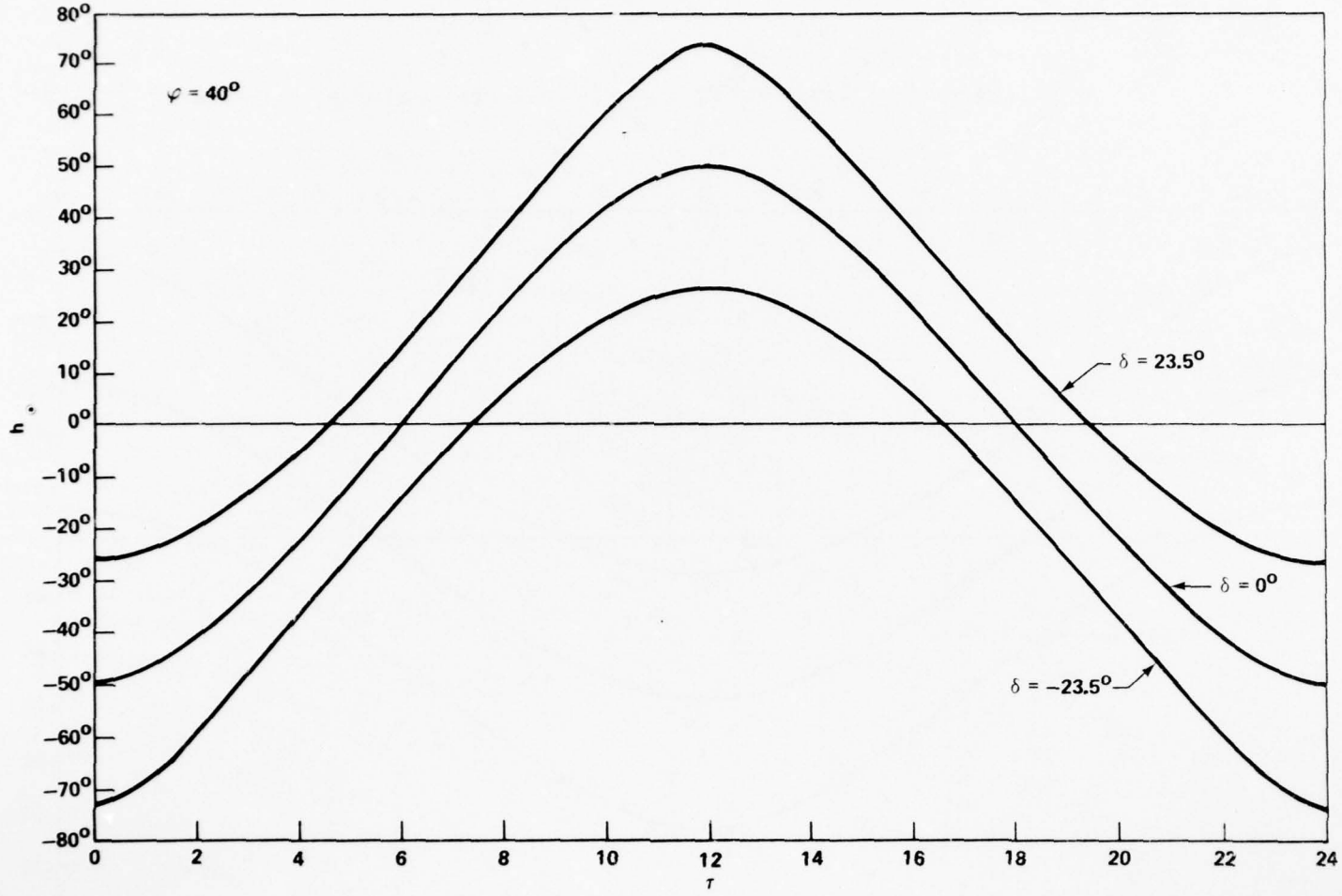

Figure 16. Change of the sun's height during a day (latitude $\varphi = 40°$).

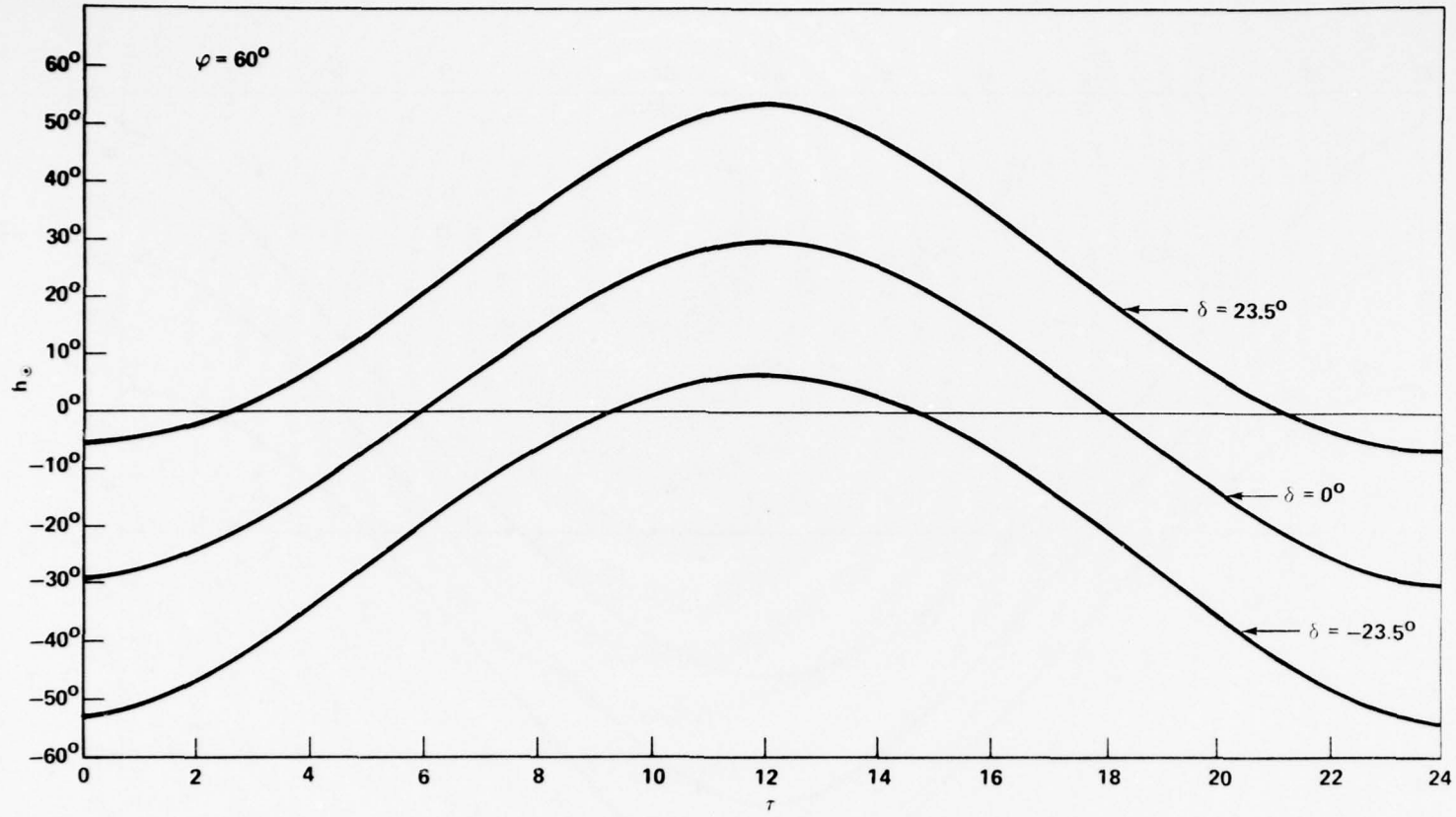

Figure 17. Change of the sun's height during a day (latitude $\varphi = 60°$).

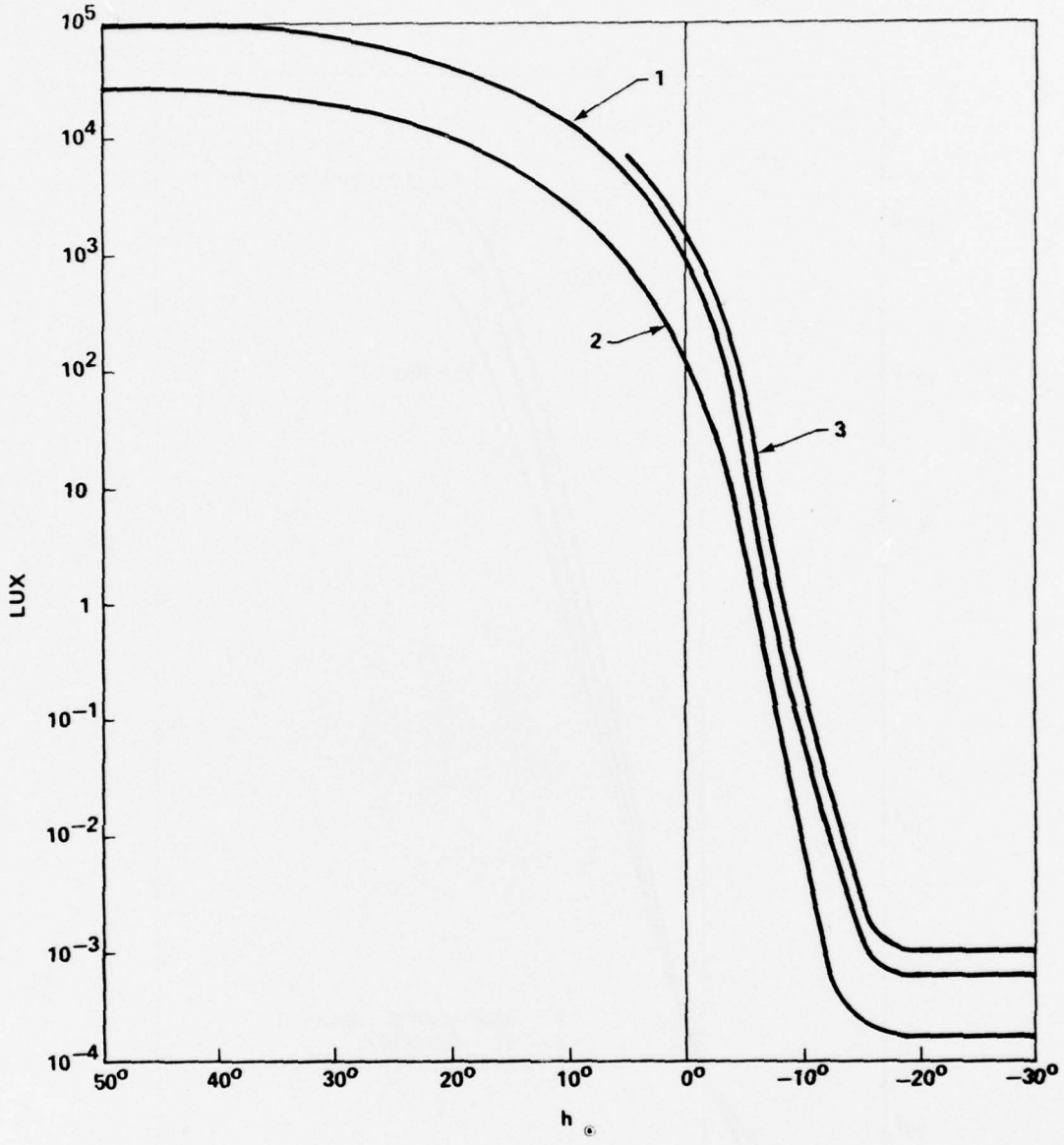

CURVE 1 – CLEAR AND UP TO 5/10 CLOUD–COVERED SKY
CURVE 2 – 10/10 CLOUD–COVERED SKY
CURVE 3 – HIGHEST BRIGHTNESS OBSERVED IN THIS TEST PERIOD

Figure 18. Brightness course of a flat horizontal plane during a day.

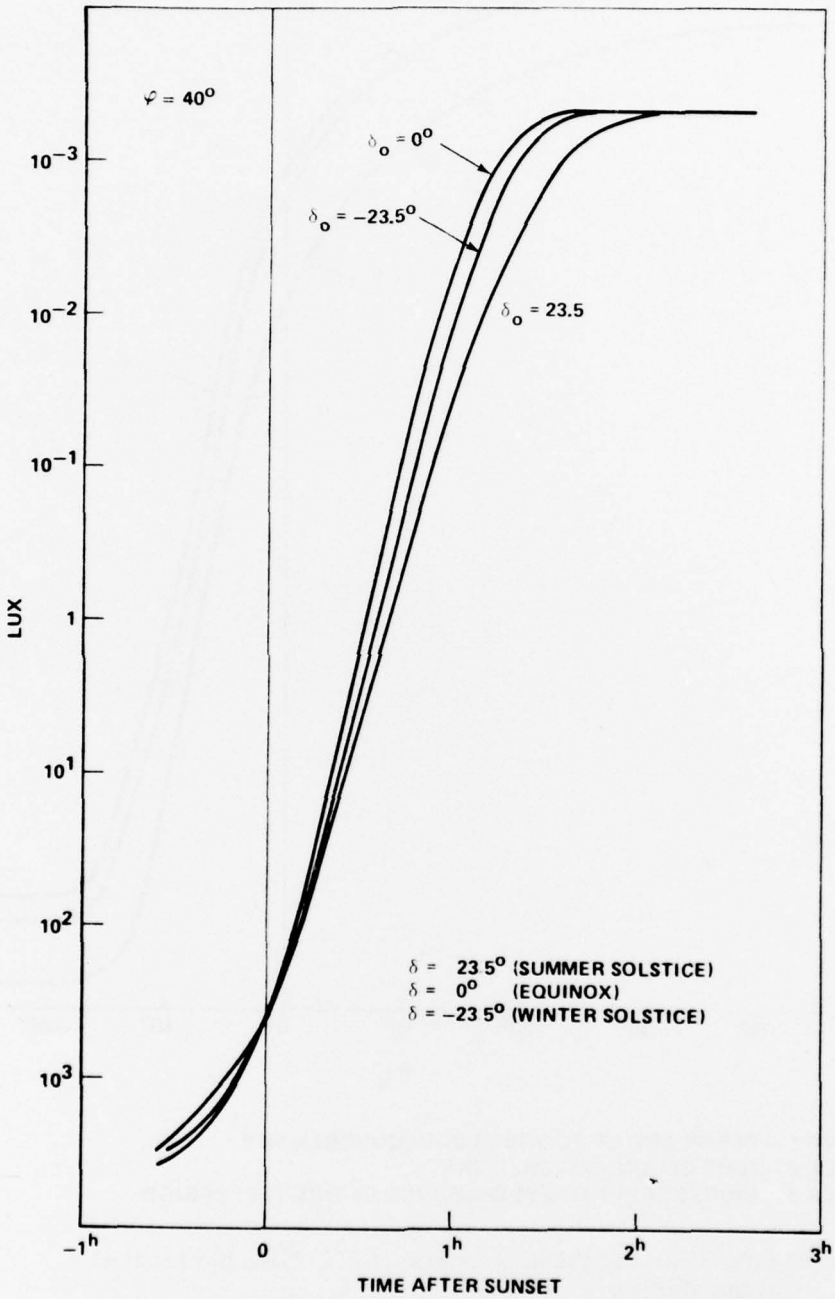

Figure 19. Brightness courses of a flat horizontal plane during dawn for geographic latitude $\varphi = 40°$ on clear and up to 5/10 cloud-covered sky.

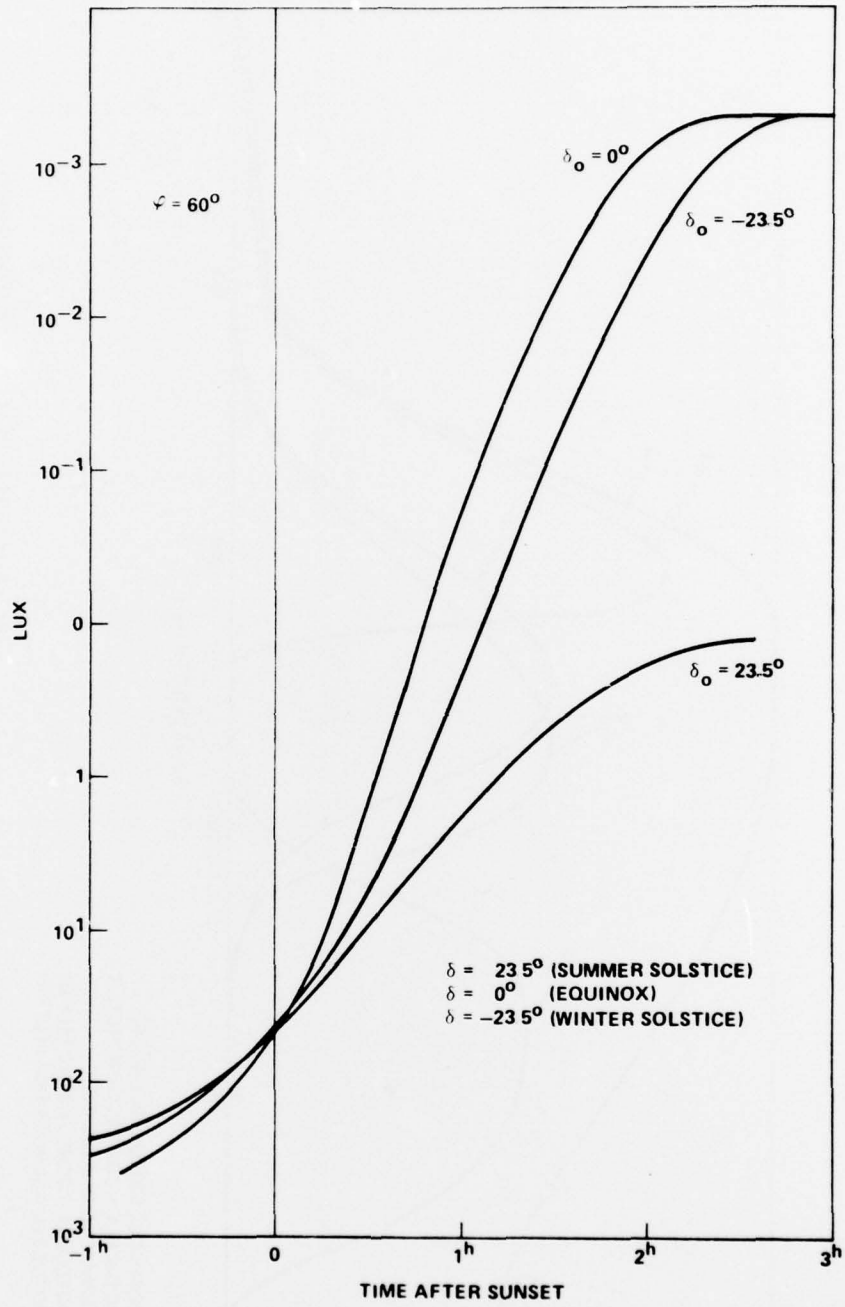

Figure 20. Brightness course of a flat horizontal plane during dawn for geographic latitude $\varphi = 60°$ on clear and up to 5/10 cloud-covered sky.

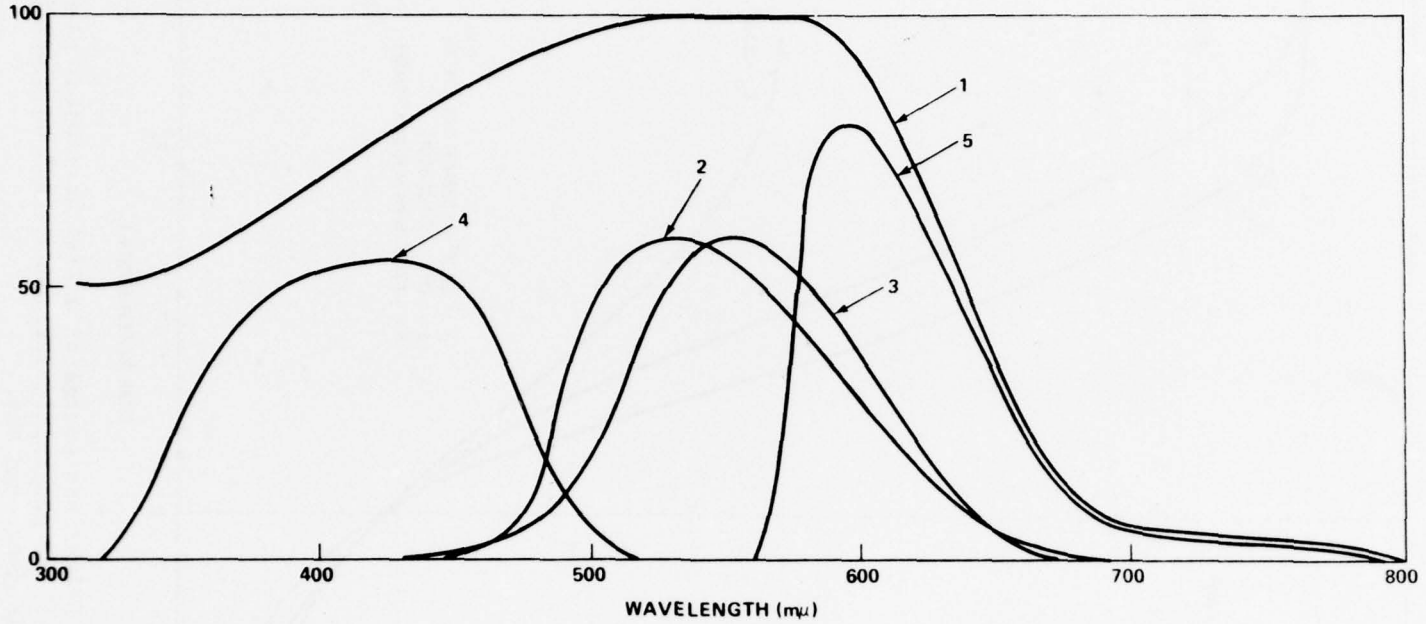

1. PHOTOCELL S50 (DR. B. LANGE)
2. PHOTOCELL + CORRECTION FILTER
3. HUMAN EYE DURING DAY
4. PHOTOCELL + SCHOTT BG12 FILTER
5. PHOTOCELL + SCHOTT OG2 FILTER

Figure 21. Spectral response of photocell and photocell-filter combinations.

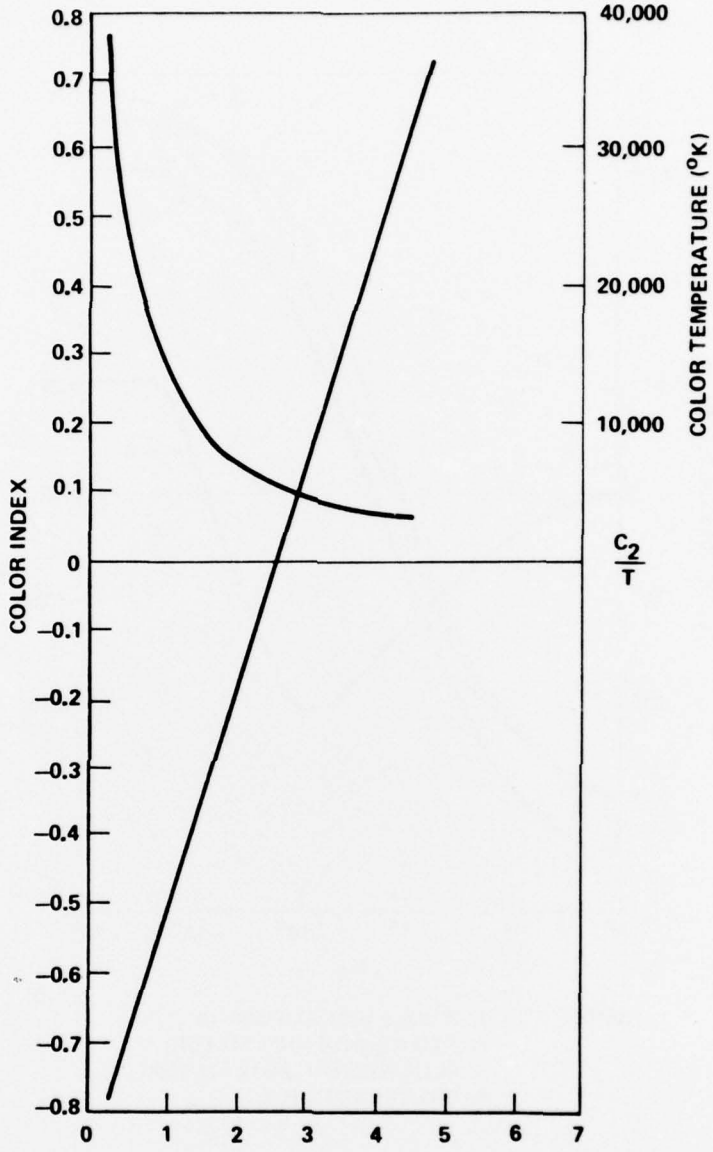

Figure 22. Relation between color index and color index temperature.

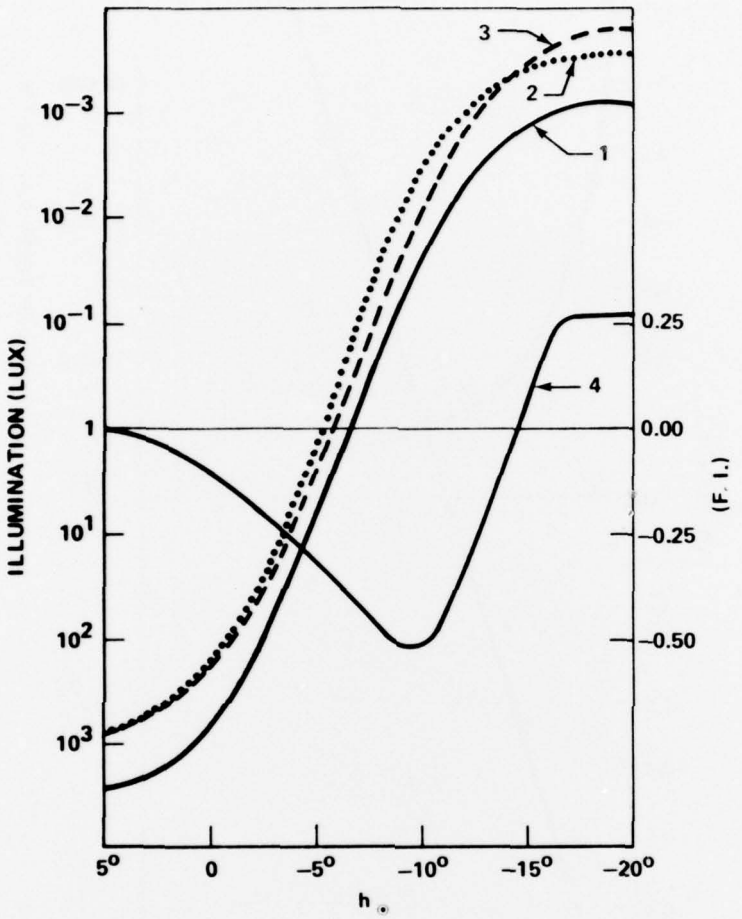

Figure 23. Brightness course of a flat horizontal plane during dawn of a cloudless day.

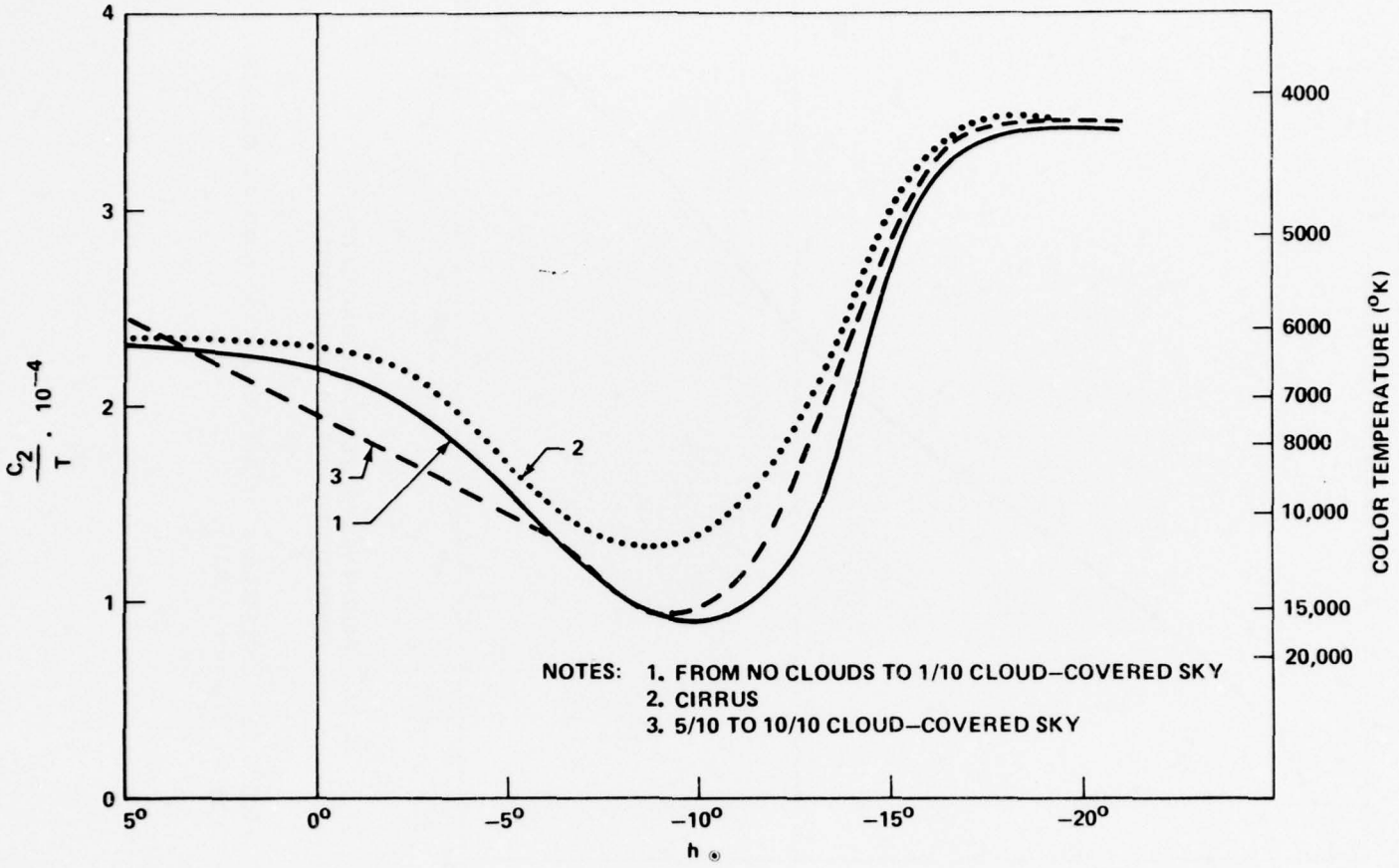

Figure 24. Course of color temperature during dawn of light received by a flat horizontal plane.

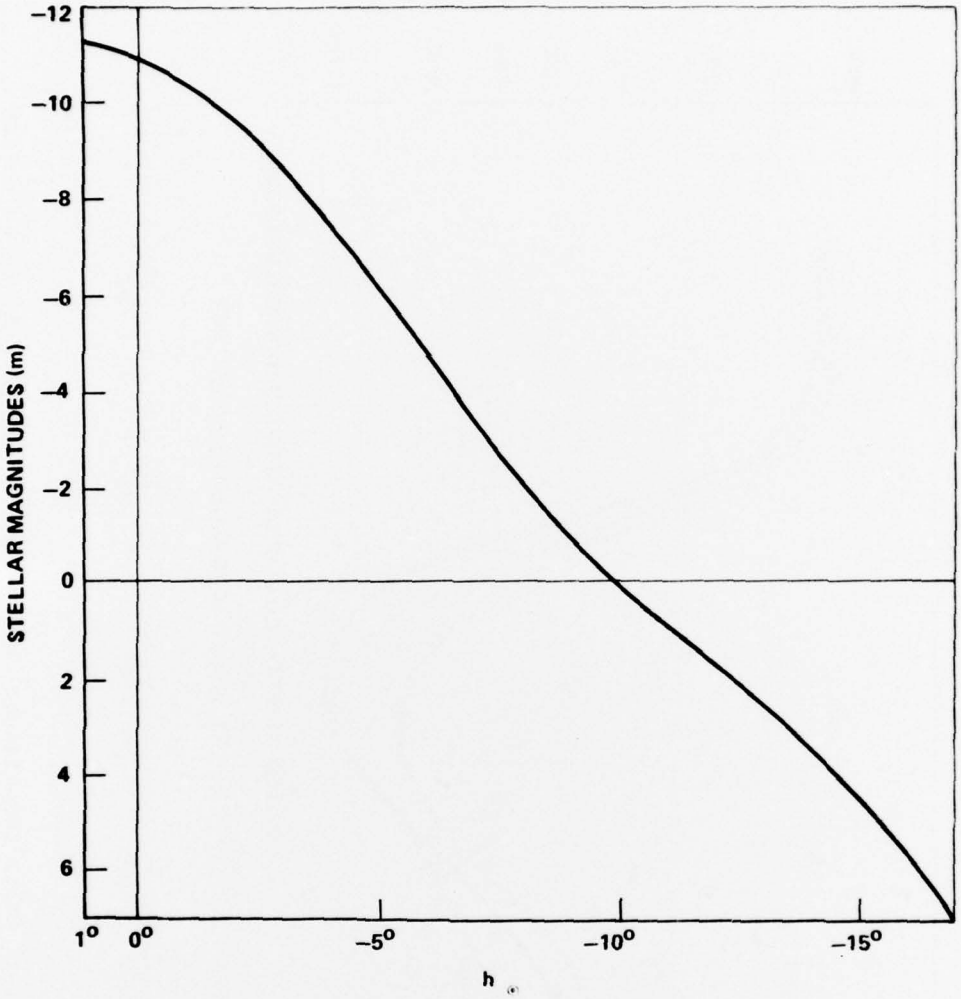

Figure 25. Brightness of zenith during dawn as measured by W. Brunner (1931).

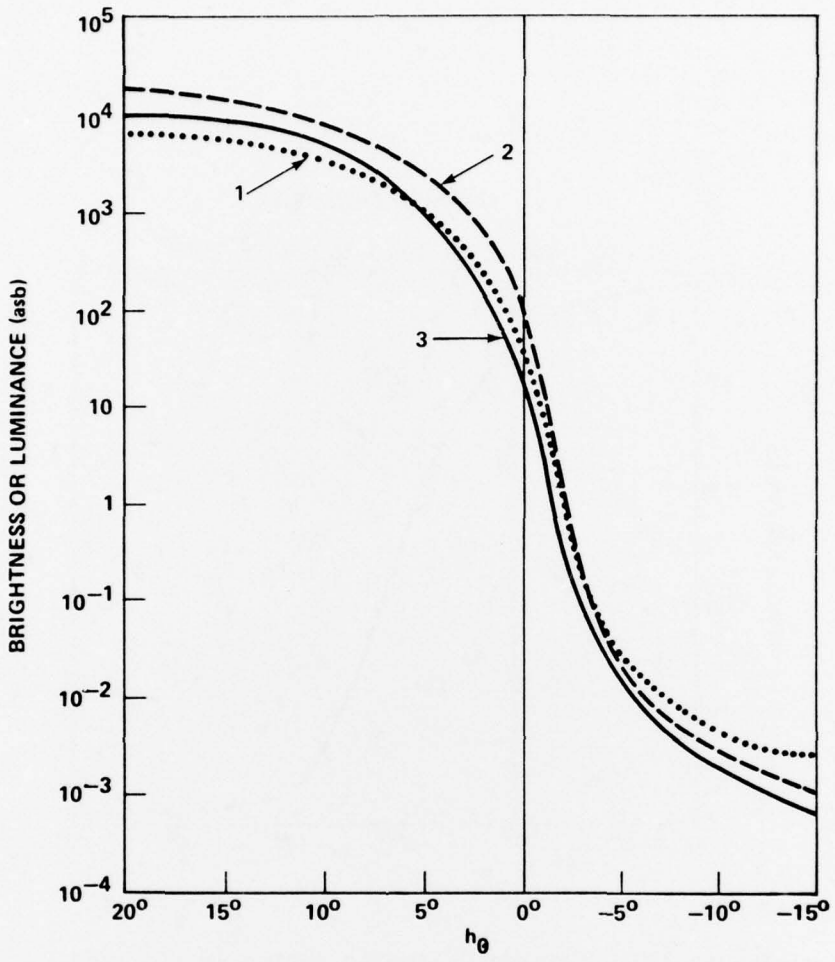

Figure 26. Course of zenith brightness and sun height as measured by K. Bullrich.

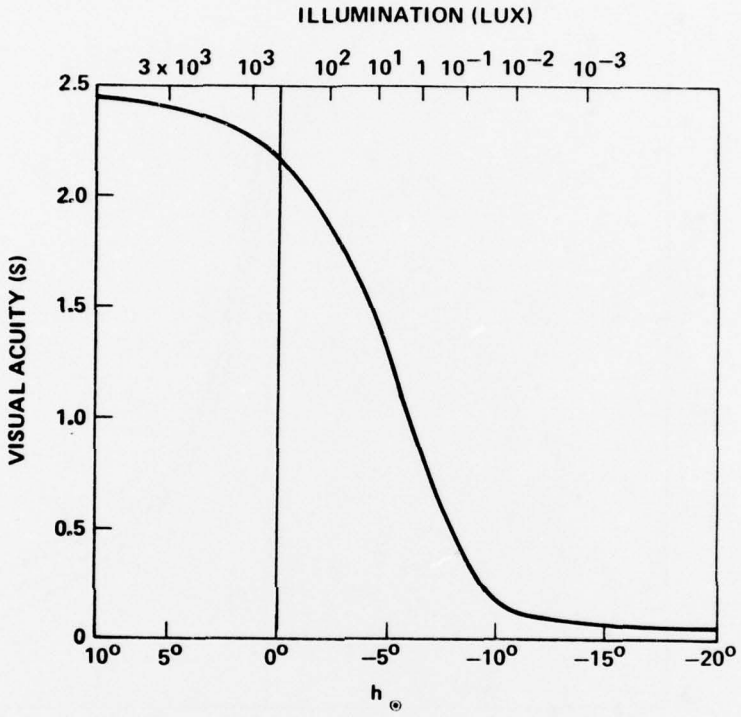

Figure 27. Decrease of acuity during dawn (Landolt test) of a day with clear to 5/10 cloud-covered sky.

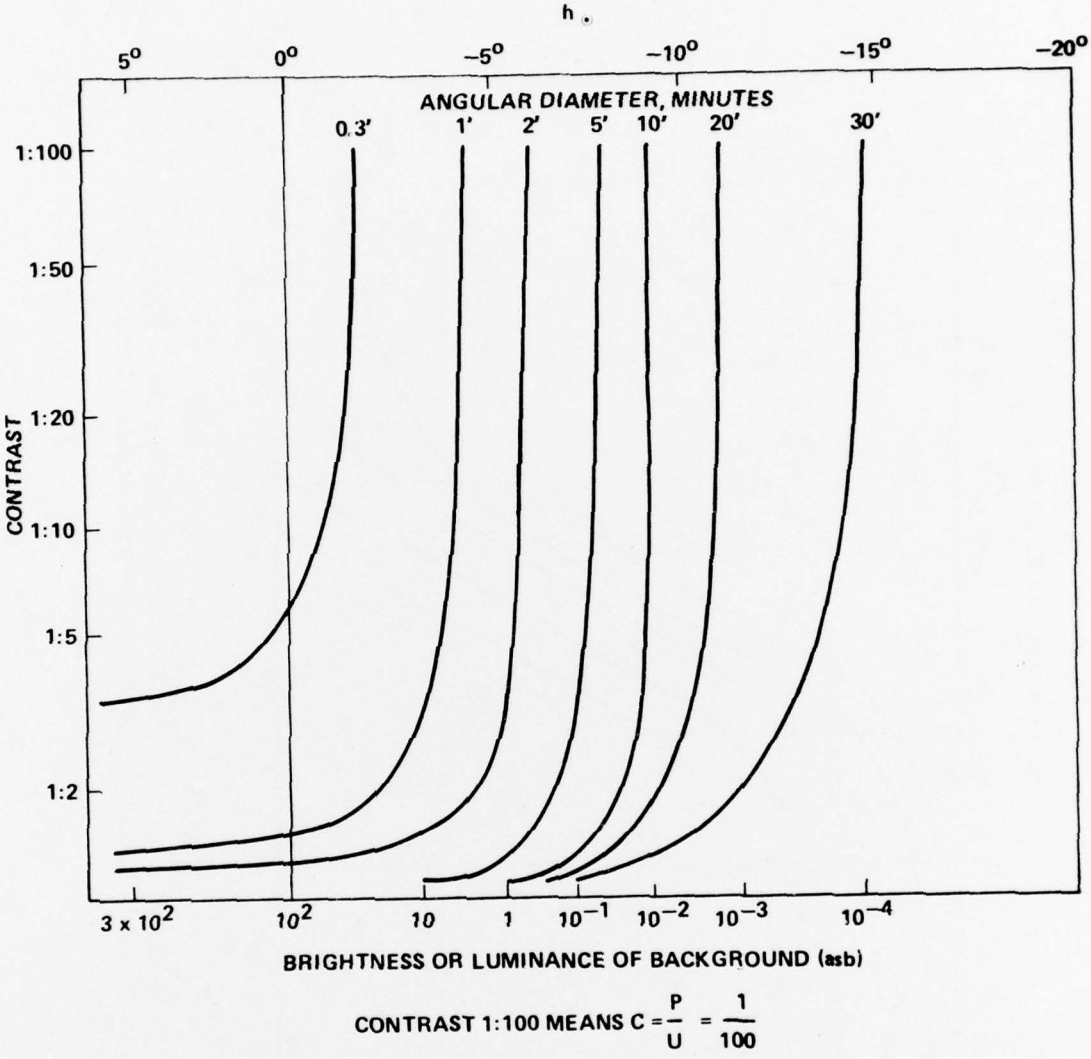

Figure 28. *Visibility thresholds* of dark objects of different diameters and contrast in open terrain of 10% reflectance during the dawn.

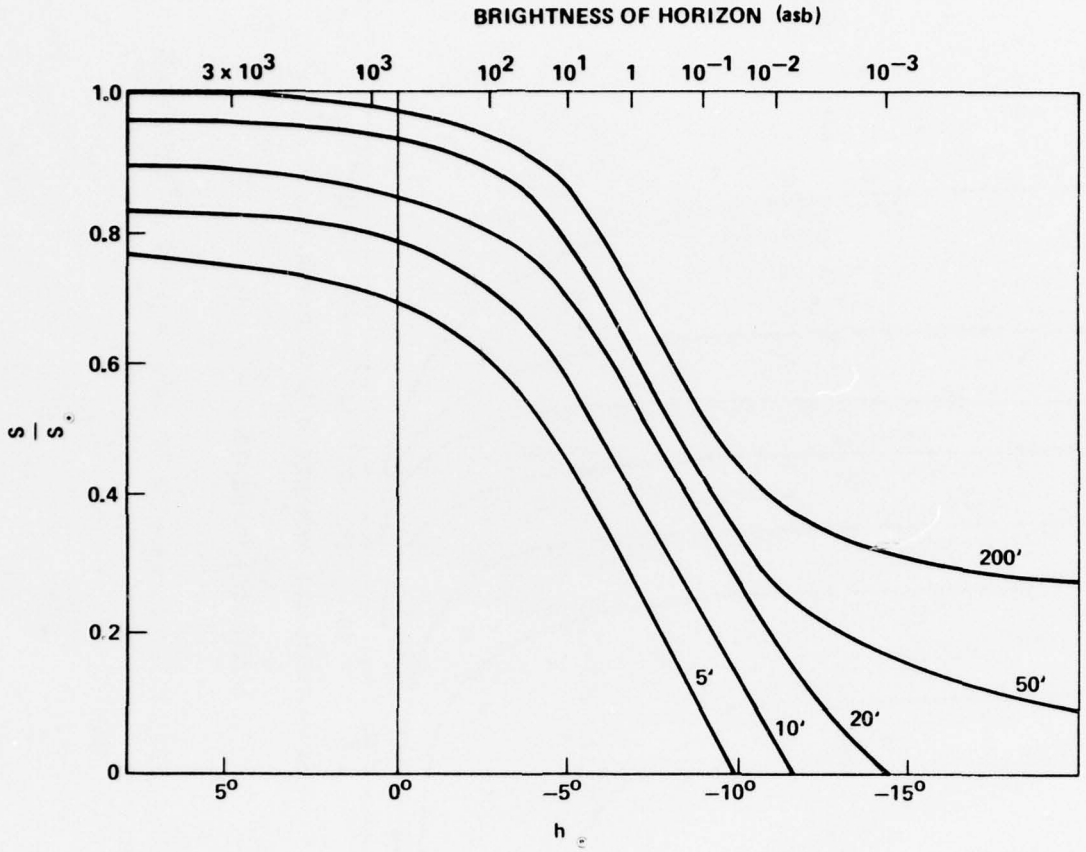

Figure 29. Visual range toward the horizon during the dawn with 6/10 to 9/10 cloud-covered sky for various angles of view (circular disk).

REFERENCES

1. Siedentopf, H., Meyer, E. J., und Wempe, J., Neue Sehschaerfemessungen, Zeitschrift fuer Instrumentenkunde, 61.11 (1941) 372-380.

2. Siedentopf, H., Neue Messungen der visuellen Kontrastschwelle, Astronomische Nachrichten, 271,5 (1941) 193-203.

3. Kuehl, A., Zur Erklaerung der Sehschaerfe mit der Beleuchtung und des absoluten Sehschaerfemaximums, Zeitschrift f. opthalmologische Optik, 28.2 (1940) 33-39.

4. Kuehl, A., Die physikalische Definition der subjektiven Helligkeit und der unbunten Farben. Zeitschrift f. technische Physik, 17.11 (1936) 439-41.

5. Nagel, M., und Klughardt, A., Die Leistung von Fernrohren bei verschiedenen Objekthelligkeiten, Zeitschrift f. Instrumentenkunde. 58 (1936) 495-502.

6. Holl, H*, Helligkeitsabfall und Farbaenderung waehrend der Daemmerung, Doctor-Thesis, University Jena, Jan. 1943.

7. Siedentopf, H., und Holl, H*, Helligkeitsabfall und Faraenderung waehrend der Daemmerung, Reichsberichte f. Physik, I (1944) 32-40.

8. Brunner, William, Beitraege zur Photometrie des Nachthimmels. Publ. d. Eidg. Sternwarte in Zuerich, Band VI (1935).

9. Bullrich, K., Met. Zeitschr. (1942) 256. Reference obtained and illustration abstracted from: Franz Linke, Handbuch der Geophysik, Band VIII, Lieferung 2, pag. 407.

10. Kimball, H. H., and associates, reference to their studies is given by: Parry Moon, The Scientific Basis of Illuminating Engineering, Dover Publications, Inc., 1961.

---

*H. Holl is synonymous with Herbert B. Holl.

DISTRIBUTION

	No. of Copies
Commander Defense Documentation Center Attn: DDC-TCA Cameron Station Alexandria, Virginia 22314	2
Commander US Army Research Office Attn: Dr. R. Lontz P. O. Box 12211 Research Triangle Park North Carolina 22709	2
US Army Research and Standardization Group (Europe) Attn: DRXSN-E-RX, Dr. Alfred K. Nedoluha Box 65 FPO New York 09510	2
US Army Materiel Development and Readiness Command Attn: Dr. Gordon Bushy Dr. James Bender Dr. Edward Sedlak 5001 Eisenhower Avenue Alexandria, Virginia 22333	1 1 1
Headquarters Hq DA (DAMA-ARZ) Washington, DC 20310	2
Director of Defense Research and Engineering Attn: Mr. L. Weisberg Washington, DC 20301	2
Director Defense Advanced Research Projects Agency 1400 Wilson Boulevard Arlington, Virginia 22209	1
Commander US Army Aviation Systems Command 12th and Spruce Streets St. Louis, Missouri 63166	1
Director US Army Air Mobility Research and Development Laboratory Ames Research Center Moffett, California 94035	1
Commander US Army Electronics Command Attn: DRSEL-TL-I, Dr. Jacobs -CT, Dr. R. Buser Fort Monmouth, New Jersey 07703	1 1
Director US Army Night Vision Laboratory Attn: John Johnson Fort Belvoir, Virginia 22060	1
Director Atmospheric Sciences Laboratory US Army Electronics Command White Sands Missile Range, New Mexico 88002	1
Director US Army Ballistic Research Laboratories Attn: Ken Richer Aberdeen Proving Ground, Maryland 21005	1
Commander US Army Combined Arms Combat Development Activity Fort Leavenworth, Kansas 66027	1
Commander US Army Frankford Arsenal Philadelphia, Pennsylvania 19137	1
Commander US Army Picatinny Arsenal Dover, New Jersey 07801	1
Commander US Army Tank Automotive Development Command Attn: DRDTA-RWL Warren, Michigan 48090	1
Commander US Army Mobility Equipment Research and Development Command Fort Belvoir, Virginia 22060	1
Commander US Army Harry Diamond Laboratories Attn: Dr. Stan Kulpa 2800 Powder Mill Road Adelphi, Maryland 20783	1
Commander US Army Armament Command Rock Island, Illinois 61202	1
Commander US Army Foreign Science and Technology Center Federal Office Building 220 7th Street, NE Charlottesville, Virginia 22901	1
Commander US Army Training and Doctrine Command Fort Monroe, Virginia 23351	1
Director Ballistic Missile Defense Advanced Technology Center Attn: ATC-D -O -R -T P. O. Box 1500 Huntsville, Alabama 35807	1 1 1 1
Commander US Naval Air Systems Command Washington, DC 20360	1
Chief of Naval Research Department of the Navy Washington, DC 20360	1
Commander US Naval Air Development Center Attn: Radar Division Warminster, Pennsylvania 18974	1
Commander US Naval Electronics Laboratory Center San Diego, California 92152	1
Commander US Naval Surface Weapons Center Dahlgren, Virginia 22448	1

	No. of Copies
Commander US Naval Weapons Center Attn: Mr. Robert Moore China Lake, California 93555	1
Director Naval Research Laboratory Attn: Code 5300, Radar Division, Dr. Skolnik Code 5370, Radar Geophysics Branch Code 5460, Electromagnetic Prop Branch Washington, DC 20390	1 1 1
Commander Rome Air Development Center US Air Force Attn: R. McMillan, OCSA James Wasielewski, IRRC Griffiss Air Force Base, New York 13440	1 1
Commander US Air Force, *AFOSR/NP* Attn: LT COL Gordon Wepfer Bolling Air Force Base Washington, DC 20332	1
Commander US Air Force Avionics Laboratory Attn: Don Rees CPT James D. Pryce, AFAL/WE Dr. B. L. Sowers, AFAL/RWI Wright Patterson Air Force Base, Ohio 45433	1 1 1
Commander AFGL Hanscom Air Force Base, Maryland 01731	1
Commander AFATL/LMT Eglin Air Force Base, Florida 32544	1
Hughes Research Laboratory Attn: Mr. Smith Mr. John F. Henry Mr. J. M. Baird 3011 Malibu Canyon Road Malibu, California 90265	1 1 1
Environmental Research Institute of Michigan Radar and Optics Division Attn: Dr. A. Kozma Dr. C. C. Aleksoff P. O. Box 618 Ann Arbor, Michigan 41807	1 1
University of Alabama Physics Department Attn: Dr. J. G. Castle 4701 University Drive, NW Huntsville, Alabama 35807	2
Institute of Defense Analysis Science and Technology Division Attn: Dr. Vincent J. Corcoran 400 Army-Navy Drive Arlington, Virginia 22202	1
Director Calspan Corporation Attn: R. Kell P. O. Box 235 Buffalo, New York 14221	1

	No. of Copies
California Institute of Technology Attn: Dr. N. George 1201 E. California Boulevard Pasadena, California	1
Optical Science Consultants Attn: Dr. D. L. Fried P. O. Box 388 Yorba Linda, California 92686	1
The Aerospace Corporation Attn: Dr. D. T. Hodges, Jr. 2350 East El Segundo Boulevard Los Angeles, California 90009	1
Commander Center for Naval Analyses Attn: Document Control 1401 Wilson Boulevard Arlington, Virginia 22209	1
Hughes Aircraft Company Missile System Group Attn: Dr. J. A. Glassman Canoga Park, California 91304	1
Goodyear Aerospace Corporation Arizona Division Attn: Mr. Fred Wilcox Mr. P. W. Murray Litchfield Park, Arizona 85340	1 1
Honeywell, Incorporated Systems and Research Division Attn: Dr. Paul Kruse Minneapolis, Minnesota 55413	1
Raytheon Company Attn: A. V. Jelalian 528 Boston Post Road Sudbury, Massachusetts 01776	1
Georgia Institute of Technology Engineering Experiment Station Attn: James Gallaper 347 Ferst Drive Atlanta, Georgia 30332	1
The Rand Corporation Attn: Dr. S. J. Dudzinsky, Jr. 1700 Main Street Santa Monica, California 90406	1
DRSMI-FR, Mr. Strickland -LP, Mr. Voigt	1 1
DRDMI-X Dr. McDaniel -T, Dr. Kobler -TBH -TC -TD -TE -TE, Mr. Pittman -TF -TG -TH -TK -TN -TR Dr. Hartman Dr. Bennett Mrs. Davis -TRE -Y -E, Mr. Lowers -ES, Mr. Pinyerd -ES, Mr. Fink -ESP, Dr. Holl -TB -TI (Record Set) (Reference Copy)	1 1 2 1 1 1 1 1 1 1 1 1 1 1 5 1 1 1 1 50 3 1 1